

# Deletion of ADAMTS5 does not affect aggrecan or versican degradation but promotes glucose uptake and proteoglycan synthesis in murine adipose derived stromal cells

Daniel J. Gorski<sup>1</sup>, Wenfeng Xiao<sup>2,5</sup>, Jun Li<sup>2</sup>, Wei Luo<sup>2,5</sup>, Mark Lauer<sup>3</sup>, John Kisiday<sup>4</sup>, Anna Plaas<sup>1,2</sup> and John Sandy<sup>1</sup>

1 - Dept. of Biochemistry, Rush Medical Center, Chicago, IL, USA

2 - Dept. of Internal Medicine (Rheumatology), Rush Medical Center, Chicago, IL, USA

3 - Lerner Research Institute, Cleveland Clinic, Cleveland, OH, USA

4 - Equine Orthopedic Research Center, College of Veterinary Medicine and Biomedical Sciences, Colorado State University, Fort Collins, CO, USA

5 - Dept. of Orthopedics, Xiangya Hospital, Central South University, Changsha, Hunan, PR China

**Correspondence to Anna Plaas:** Department of Internal Medicine (Rheumatology), 1611 W. Harrison St. Suite 510, Chicago, IL 60612, USA. [Anna\\_Plaas-Sandy@rush.edu](mailto:Anna_Plaas-Sandy@rush.edu)  
<http://dx.doi.org/10.1016/j.matbio.2015.03.008>

## Abstract

ADAMTS5 (TS5), a member of the aggrecanase clade (TS1, 4, 5, 8, 9, 15) of ADAMTS-proteases, has been considered largely responsible for the proteolysis of the hyalactans, aggrecan (Acan) and versican (Vcan), in vivo. However, we have reported that *ts5*-knockout (KO) mice show joint protection after injury due to inhibition of synovial scarring and enhanced Acan deposition. Also, KO mice have an impaired wound healing phenotype in skin and tendons which is associated with Acan/Vcan-rich deposits at the wound sites. Moreover, the Acan and Vcan deposited was aggrecanase-cleaved, even in the absence of TS5. In this study, we have used adipose-derived stromal cell (ADSC) and epiphyseal chondrocyte cultures from wild type and KO mice to further study the role of TS5 in Acan and Vcan turnover. We have confirmed with both cell types that the aggrecanase-mediated degradation of these hyalactans is not due to TS5, but an aggrecanase which primarily cleaves them before they are secreted. We also provide data which suggests that TS5 protein functions to suppress glucose uptake in ADSCs and thereby inhibits the synthesis, and promotes the intracellular degradation of Acan and Vcan by an ADAMTS other than TS5. We propose that this apparently non-proteolytic role of TS5 explains its anti-chondrogenic and pro-fibrotic effects in murine models of wound repair. A possible role for TS5 in an endocytotic process, involving competitive interactions between TS5, LRP1 and GLUT4 is discussed.

© 2015 Published by Elsevier B.V. This is an open access article under the CC BY-NC-ND license (<http://creativecommons.org/licenses/by-nc-nd/4.0/>).

## Introduction

Multipotent connective tissue progenitor cells, also known as mesenchymal stem cells (MSCs), have been identified in skin [1] and tissues of the musculoskeletal system [2] as well as in the stroma of most tissues and organs, including bone marrow, brain, kidney, liver, thymus, kidney glomeruli, muscle, lung and adipose tissue [3]. They are emerging as major effectors in healing, since they proliferate

and differentiate to cells which can regenerate a functional location-specific repair tissue [4], such as a collagen type I/III rich ECM in the dermis, a calcified ECM matrix at fracture sites, an aggrecan/type II collagen-rich ECM in cartilage or a mucoid-rich ECM in the respiratory and gastro-intestinal systems.

In the development of cell-based regenerative medicine [5], ADSCs [6,7] have gained popularity for clinical usage, due to their ready availability compared to autologous bone marrow derived MSCs [8]

0022-2836/© 2015 Published by Elsevier B.V. This is an open access article under the CC BY-NC-ND license (<http://creativecommons.org/licenses/by-nc-nd/4.0/>). *Matrix Biol.* (2015) xx, xxx–xxx

Please cite this article as: Gorski Daniel J., et al, Deletion of ADAMTS5 does not affect aggrecan or versican degradation but promotes glucose uptake and proteoglycan synthesis in mur..., *Matrix Biol.* (2015), <http://dx.doi.org/10.1016/j.matbio.2015.03.008>

and umbilical cord blood stem cells [9]. In the undifferentiated state, progenitor cells express characteristic cell surface molecules [10] and produce a pericellular ECM, both in vivo and in vitro [11–13]. This ECM, composed of a network of fibrillar proteins, hyaluronan and proteoglycans, provides cellular protection from host-rejection [14] and can alter responsiveness to differentiation factors, such as TGF $\beta$ s/BMPs, Wnt/ $\beta$ -Catenin and Notch [12]. For example, decorin, biglycan, betaglycan and laminin [15,16] can sequester growth factors of the TGF $\beta$ -superfamily; heparan sulfate proteoglycans of the syndecan and glypican families [17] enhance FGF2 dependent signaling [18] and CD44–HA interactions [19] can facilitate TGF- $\beta$ 1 signaling processes [20].

The hyalactans, Vcan and Acan have also been described in the ECM of MSCs and adipose stromal cells [21–25] but their precise roles are unclear. Some insight was provided by developmental studies with *ts5*<sup>-/-</sup> mice suggesting that Vcan accumulates due to a loss of TS5 activity, promotes the fibroblast–myofibroblast transition [26] and is associated with mesenchymal cell proliferation in myxomatous heart valves [27] and myoblast fusion [28]. Also, our work on soft-tissue wound healing found that an accumulation of Acan/Vcan in the ECM of *ts5*<sup>-/-</sup> mice prevented TGF $\beta$ -dependent SMAD2/3 signaling [29]. We have now extended these studies to examine the role of TS5 in Acan and Vcan turnover in ADSCs from WT and *ts5*<sup>-/-</sup> mice, using chondrocyte cultures as a control for Acan secretion and processing. We present data to suggest that TS5 reduces the hyalactan content of the pericellular ECM by inhibiting the synthesis and secretion of Acan and Vcan. This modulatory function of TS5 appears to operate by decreasing the cellular uptake of glucose, rather than through the presumed proteolytic degradation of hyalactans.

## Results

### Genotyping and mRNA analysis of two strains of *ts5*<sup>-/-</sup> mice

Two lines of *ts5*<sup>-/-</sup> mice in the C57BL/6 background were compared. Both were generated by deletion of exon 2 which encodes the catalytic site. One was from Lexicon (characterized in [30], and herein called *ts5*<sup>-/-</sup>P) and the other from the Jackson laboratory (characterized in [31] and herein called *ts5*<sup>-/-</sup>J [27]). The genomic PCR product was 642 bp for WT, 374 bp for *ts5*<sup>-/-</sup>P DNA and no product was detected in *ts5*<sup>-/-</sup>J (Fig. 1D), confirming deletion of exon 2 in both KO strains. For *ts5*<sup>-/-</sup>J, deletion of exon 2 and the insertion of a LacZ + Neo cassette was also confirmed (WT and *ts5*<sup>-/-</sup>P products at 271 bp and

*ts5*<sup>-/-</sup>J product at 424 bp) with Jackson Lab protocols (Fig. 1E). mRNA transcripts in ADSCs from the three genotypes were analyzed with primers targeting exons 1 and 4 (Fig. 1B, primer set 'I'). This showed the expected 475 bp product in WT cells and its absence in *ts5*<sup>-/-</sup>J cells, but an unexpected transcript at 342 bp in *ts5*<sup>-/-</sup>P cells (Fig. 1B, F). This was confirmed by generation of a 277 bp product with primers to an overlapping sequence generated by fusion of exons 1 and 3 (Fig. 1F, primer set 'II'). In comparison, PCR for transcripts in *ts5*<sup>-/-</sup>J cells with primer set 'II' gave no product, consistent with the reported out-of-frame deletion in this KO strain (Fig. 1F). Analysis of *ts5*<sup>-/-</sup>P mRNA with primers for exons 1 and 8 (Fig. 1G, primer set 'III'), showed the presence of a 2.8 kB lacking exon 2 in ADSC cultures. Identification of these PCR products was confirmed by sequencing (data not shown). In summary, this showed that the *ts5*<sup>-/-</sup>P mice contained an in-frame deletion of exon 2, which was not reported previously [30].

### Western analysis of TS5 protein in tissue extracts, ADSCs and serum

TS5 protein was analyzed with antibodies to the catalytic domain and the cys-rich region (see schematic, Fig. 2D, for putative TS5 structures and epitope locations). WT skeletal muscle contained a 40 kDa species that reacted with both  $\alpha$ -cat and  $\alpha$ -cys and, as expected, was not detected in equivalent samples from *ts5*<sup>-/-</sup>P or *ts5*<sup>-/-</sup>J mice (Fig. 2A). Its migration behavior, relative to recombinant TS5 standards [32] suggests that it is an inactive species formed by removal of the pro-domain by furin-like activity (R261/S262) and C-terminal truncation at a site including at least part of the cys-rich region epitope (residues 636–649). The structure of the strong  $\alpha$ -cys-reactive band at ~120 kDa in WT (but not in *ts5*<sup>-/-</sup>P or *ts5*<sup>-/-</sup>J) muscle extracts is unknown, but it might represent the pro-form of TS5. Extracts from WT ADSC cultures showed TS5 species at 38 kDa and 34 kDa (Fig. 2B) and neither was present in *ts5*<sup>-/-</sup>P or *ts5*<sup>-/-</sup>J extracts, consistent with their identification as TS5 fragments. In addition, a 75 kDa species, which reacted strongly with the  $\alpha$ -cys domain antibody, was present in all ADSC samples and this was found to be from the serum (Fig. 2C). To our knowledge, this is the first characterization of TS5 protein species that are present in WT mice and undetectable in the equivalent KO samples.

### Analysis of MSC marker gene expression in ADSCs and chondrocytes

Both cell types were examined for expression of putative marker genes for MSCs (Cd73, Cd93, and

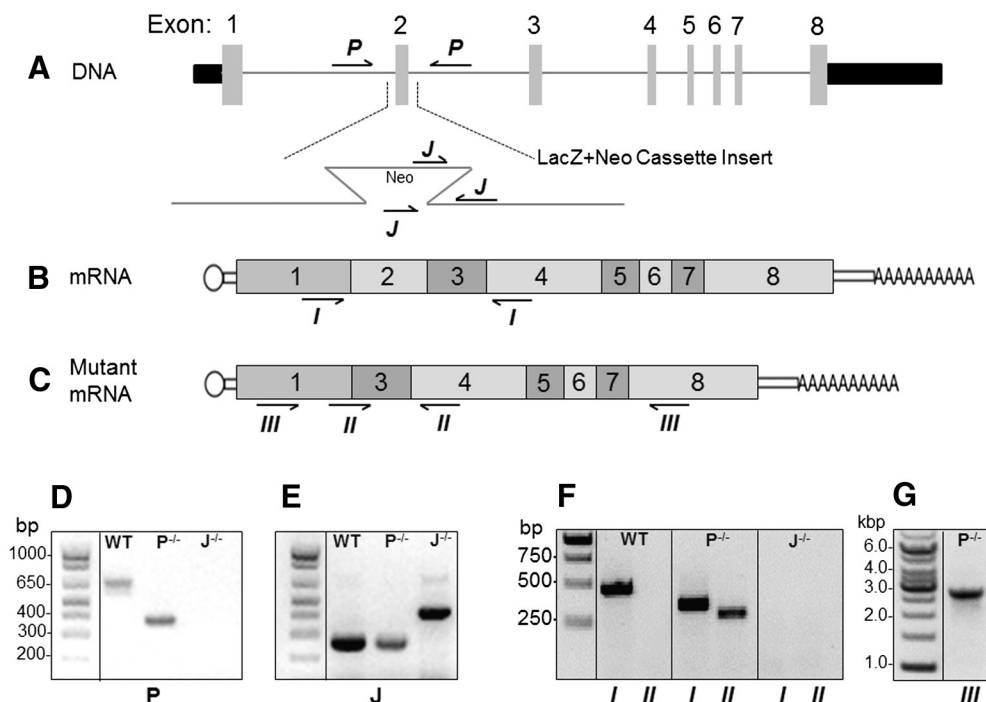


**Fig. 1.** Genotyping and mRNA analysis. (A) Diagram of TS5 gene showing primer locations for genotyping  $ts5^{-/-}P$  ( $P^{-/-}$ ) and  $ts5^{-/-}J$  ( $J^{-/-}$ ) mice. (B) Diagram of full length WT *Adamts5* mRNA showing locations of primer set 'I'. (C) Diagram of mutant mRNA with exon 2 deletion, showing locations of primer set 'II' and 'III'. (D) PCR products from genotyping WT,  $ts5^{-/-}P$  and  $ts5^{-/-}J$  cells with primer set 'P'. (E) PCR products from genotyping WT,  $ts5^{-/-}P$  and  $ts5^{-/-}J$  cells with primer set 'J'. (F) PCR products amplified with cDNA from WT,  $ts5^{-/-}P$  and  $ts5^{-/-}J$  cells with primer sets 'I' and 'II'. (G) PCR products amplified with cDNA, from  $ts5^{-/-}P$  cells, with primer set 'III'.

Cd105 [33]) and murine phagocytotic cells (F4/80 [34]) (Table 1). WT ADSCs expressed these genes in the following order of abundance: Cd90 > Cd105 > Cd73 » F4/80. Interestingly their expression was also seen in primary high density monolayers of WT chondrocytes, and found to be at similar expression levels for Cd90 and Cd105 but higher expression for Cd73 and F4/80 compared to ADSCs. This is likely due to the presence in chondrocyte cultures, of a second cell type, with a flattened morphology, similar to that characteristic of ADSC cultures (Fig. S-1C).

Some minor, yet statistically significant changes were seen, when comparing expression levels of the marker genes between cells from the different genotypes. Thus, abundance of transcripts for Cd73 and Cd90 were lower in  $ts5^{-/-}J$  than in either WT or  $ts5^{-/-}P$  ADSCs; Cd105 was higher in  $ts5^{-/-}P$  than WT or  $ts5^{-/-}J$  ADSCs. Furthermore, in chondrocyte cultures, Cd90 was higher in  $ts5^{-/-}J$  than WT or  $ts5^{-/-}P$  and F4/80 expression was higher in both  $ts5^{-/-}P$  and  $ts5^{-/-}J$  compared to WT chondrocytes. The biological significance of such distinctions is currently unknown, but could be due to variability of cell responses to isolation and maintenance often seen in primary cell cultures.

### Characterization of ADSCs and chondrocytes by ECM gene expression

The expression of fibroblast and chondrocyte specific ECM genes in both cell types was determined for WT,  $ts5^{-/-}P$ , and  $ts5^{-/-}J$  cells (Table 2). Consistent with their stromal origin, all ADSCs expressed *Col1a1*, *Col3a1*, *Has1* and *Has2*, but *Col2a1*, and *Acan* were essentially below detection. Conversely chondrocytes from all three genotypes strongly expressed *Col2a1* and *Acan*. Notably, transcript abundance for *Col1a1* and *Col3a1*, was also high in all chondrocytes, and this is likely due to the fibroblast-like cells in the chondrocyte cultures (Fig. S-1C).

Expression levels of ECM genes in both ADSCs and chondrocytes were clearly affected by the phenotype. Thus, *Col1a1* and *Col3a1* in ADSCs were lower in both KOs than WT, and *Col2a1* in chondrocytes was also markedly decreased in both KOs, in support of our observation that TS5 is required for robust expression of fibrillar collagens [29]. Expression of genes for assembly of a glyco-matrix (*Vcan V1* (previously called *V0*) and *V2* (previously *V1*)), were not influenced by *ts5* ablation per se, but *Has1* and *Has2* expression was elevated in  $ts5^{-/-}P$  compared  $ts5^{-/-}J$  or WT ADSCs.

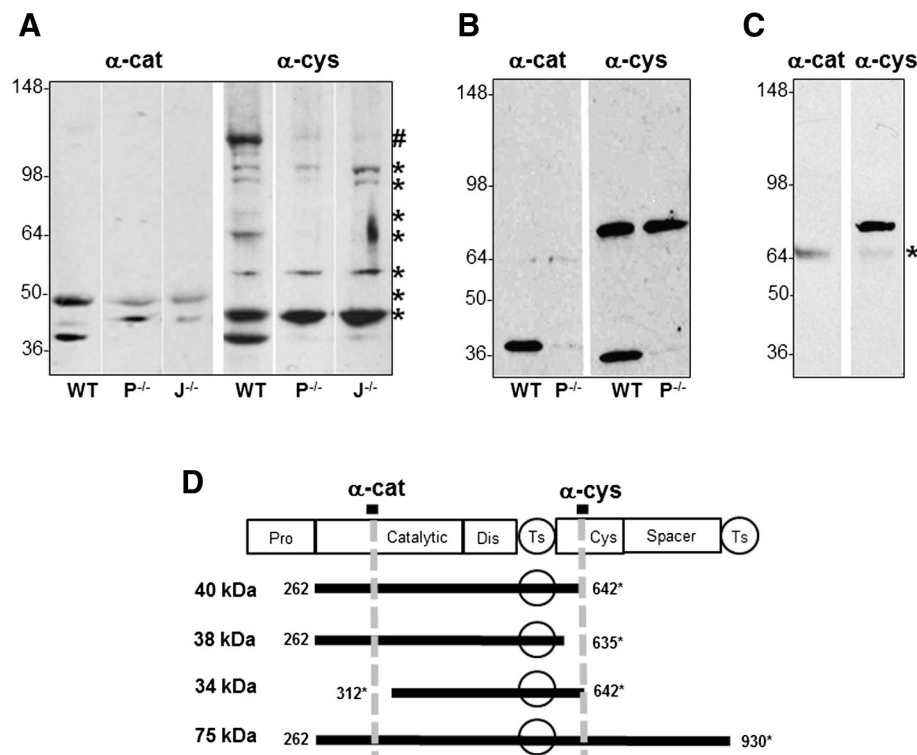


**Fig. 2.** Western analysis of ADAMTS5 in muscle, ADSC cultures and fetal bovine serum. Western blots of skeletal muscle extract (A), ADSC cell layers (B) and FBS (C) used for cell culture were probed with antibodies raised against the catalytic domain ( $\alpha$ -cat) or cysteine rich domain ( $\alpha$ -cys) of human ADAMTS5. (D) Schematic representation of ADAMTS5 with epitope locations and putative fragment structures. Asterisks (\*) denotes non-specific bands (#) denotes uncharacterized band.

Expression of *Vcan V2* in chondrocytes was higher in WT and *ts5<sup>-/-</sup>J* compared to *ts5<sup>-/-</sup>P* and expression of *Has2* in chondrocyte was decreased in *ts5<sup>-/-</sup>J* relative to *ts5<sup>-/-</sup>P*. The importance of these genotypic differences is unknown but likely due to variations in culture adaptation of cells from the different genotypes.

#### CS/DS and HA production by ADSCs from WT, *ts5<sup>-/-</sup>P* and *ts5<sup>-/-</sup>J* mice

Cell layers and 24 h conditioned medium from confluent cultures of WT, *ts5<sup>-/-</sup>P* and *ts5<sup>-/-</sup>J* cells were analyzed for CS/DS and HA. No major difference between genotypes was detected in the total amounts of CS/DS (~25 ng/ $\mu$ g DNA/24 h) secreted into the medium (Fig. 3A) or deposited in the cell layer (~60 ng/ $\mu$ g DNA/24 h) (Fig. 3B) and the CS/DS was predominantly (>80%) 4-sulfated, with the remainder 6-sulfated. However, it was noted on FACE analysis that 6-sulfation was significantly elevated in *ts5<sup>-/-</sup>P* ADSCs, which produced ~25 ng C6S/ $\mu$ g DNA/24 h, compared to ~9 ng/ $\mu$ g DNA/24 h for either WT and *ts5<sup>-/-</sup>J* ADSCs respectively.

*ts5<sup>-/-</sup>P* cells secreted markedly more HA into the cell layer and the medium than did WT or *ts5<sup>-/-</sup>J*

cultures. Notably, the high HA level for *ts5<sup>-/-</sup>P* ADSCs was accompanied by an ~3-fold increase in mRNA transcript abundance for both *Has1* and *Has2* relative to WT or *ts5<sup>-/-</sup>J* (Table 2). Staining of cultures for HA (Fig. 3C, top row) showed that for all

**Table 1.** mRNA transcript abundance of cell surface markers in ADSC and chondrocyte cultures

| Gene  | ADSCs                     |                              |                           | Chondrocytes   |                           |                              |
|-------|---------------------------|------------------------------|---------------------------|----------------|---------------------------|------------------------------|
|       | WT                        | <i>ts5<sup>-/-</sup>P</i>    | <i>ts5<sup>-/-</sup>J</i> | WT             | <i>ts5<sup>-/-</sup>P</i> | <i>ts5<sup>-/-</sup>J</i>    |
| Cd73  | 3.1 <sup>a</sup><br>(0.7) | 2.6<br>(2.3)                 | 2.0 $\ddagger$<br>(0.4)   | 24.3<br>(8.45) | 24.3<br>(1.61)            | 28.7<br>(4.70)               |
| Cd90  | 20.8<br>(2.39)            | 34.6<br>(26.39)              | 14.1 $\ddagger$<br>(1.32) | 12.5<br>(2.84) | 10.8<br>(1.76)            | 21.4 $\ddagger$ ,*<br>(2.07) |
| Cd105 | 14.3<br>(1.4)             | 44.3 $\ddagger$ ,*<br>(23.7) | 16.0<br>(2.61)            | 20.1<br>(5.00) | 15.8<br>(1.65)            | 16.5<br>(0.90)               |
| F4/80 | 0.12<br>(0.10)            | 0.29<br>(0.15)               | 0.20<br>(0.06)            | 1.7<br>(0.03)  | 3.7 $\ddagger$<br>(0.39)  | 5.4 $\ddagger$ ,*<br>(0.93)  |

Statistically significant differences with  $p < 0.05$  are indicated for comparisons between WT and *ts5<sup>-/-</sup>P* or *ts5<sup>-/-</sup>J* as [ $\ddagger$ ] or between *ts5<sup>-/-</sup>P* and *ts5<sup>-/-</sup>J* as (\*).

<sup>a</sup> Values are given as relative mRNA abundance, calculated as ( $2^{-\Delta\text{Ct}}$ ) \* 1000 (arbitrary units),  $\Delta\text{Ct}$  relative to *Gapdh*. Values shown represent the mean ( $\pm$ SD),  $n = 6$ , 3 replicates from 2 experiments.

**Table 2.** mRNA transcript abundance for ECM genes in ADSC and chondrocyte cultures

| Gene    | WT                           |                  | <i>ts5</i> <sup>-/-P</sup>     |                              | <i>ts5</i> <sup>-/-J</sup>    |                              |
|---------|------------------------------|------------------|--------------------------------|------------------------------|-------------------------------|------------------------------|
|         | ADSC                         | CHON             | ADSC                           | CHON                         | ADSC                          | CHON                         |
| Col1a1  | 1750 <sup>a</sup><br>(228.3) | 5250<br>(980.3)  | 1173 <sup>‡,*</sup><br>(484.3) | 4427*<br>(488.0)             | 1103 <sup>‡</sup><br>(194.3)  | 988 <sup>‡</sup><br>(1153.5) |
| Col3a1  | 240.7<br>(56.81)             | 544.8<br>(223.4) | 125.9 <sup>‡</sup><br>(59.52)  | 335.2<br>(84.81)             | 106.2 <sup>‡</sup><br>(26.07) | 467.0<br>(58.59)             |
| Col2a1  | ND <sup>b</sup>              | 49.25<br>(23.67) | ND                             | 21.04 <sup>‡</sup><br>(1.36) | ND                            | 16.01 <sup>‡</sup><br>(3.83) |
| Acan    | 0.01<br>(0.003)              | 67.33<br>(16.33) | ND                             | 59.21<br>(4.87)              | ND                            | 23.78 <sup>‡</sup><br>(8.73) |
| Vcan V2 | 1.40<br>(0.43)               | 5.49<br>(0.96)   | 1.60<br>(0.80)                 | 4.35*<br>(0.71)              | 1.70<br>(0.53)                | 2.47 <sup>‡</sup><br>(0.64)  |
| Has1    | 0.46<br>(0.09)               | 0.16<br>(0.05)   | 1.28 <sup>‡</sup><br>(0.95)    | 0.17<br>(0.04)               | 0.13<br>(0.07)                | 0.21<br>(0.02)               |
| Has2    | 1.80<br>(0.43)               | 2.96<br>(0.26)   | 6.18 <sup>‡,*</sup><br>(2.13)  | 3.21*<br>(0.08)              | 1.81<br>(1.04)                | 1.57 <sup>‡</sup><br>(0.17)  |

Statistically significant differences with  $p < 0.05$  are indicated for comparisons between WT and *ts5*<sup>-/-P</sup> or *ts5*<sup>-/-J</sup> as [‡] or between *ts5*<sup>-/-P</sup> and *ts5*<sup>-/-J</sup> as (\*).

<sup>a</sup> Values are given as relative mRNA abundance, calculated as  $(2^{-\Delta Ct}) * 1000$  (arbitrary units),  $\Delta Ct$  relative to *Gapdh*. Values shown represent the mean ( $\pm$ SD),  $n = 6$ , 3 replicates from 2 experiments.

<sup>b</sup> ND = not detected, Ct value > 34.

three genotypes, it was in localized in 'capped structures' associated with cells of epithelioid morphology, and also distributed throughout the ECM of fibroblast-like cells. Notably, *ts5*<sup>-/-P</sup> cultures showed a denser staining of 'string-like' networks extending between cell groups, which might explain the increased HA content of these cultures. Vcan (Fig. 3C, second row) showed a widespread distribution with some structures organized into dense fibrillar aggregates reminiscent of those reported for fibronectin accumulation in fibroblastic cells [35,36]. Notably, despite the undetectable levels of mRNA for *Acan* in ADSCs (Table 2), core protein was readily detected, and its distribution was clearly distinct from both Vcan and HA, in that only epithelioid cell groups stained positive (Fig. 3C, third row). *Streptomyces hyaluronidase* pretreatment (data not shown) eliminated HA and Vcan reactivity from the fibroblastic regions of the cultures, but it did not affect the HA or Acan staining of the epithelioid cells, suggesting a localization, perhaps intracellular, that is not accessible to digestion by the hyaluronidase.

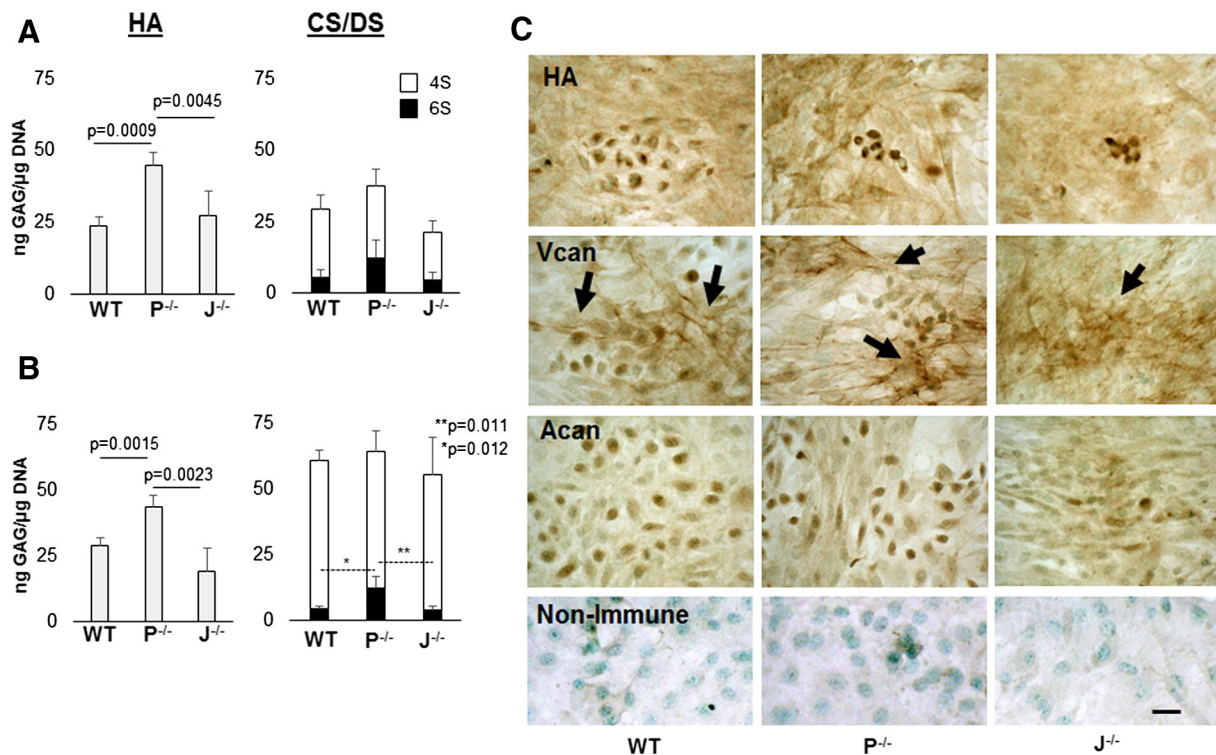


**Fig. 3.** Analysis of glyco-matrix by FACE and immunohistochemistry. Media (A) and cell layers (B) of ADSC cultures from WT, *ts5*<sup>-/-P</sup> (P<sup>-/-</sup>) and *ts5*<sup>-/-J</sup> (J<sup>-/-</sup>) mice were analyzed for chondroitin/dermatan sulfate (CS/DS) and hyaluronan (HA). Sulfated disaccharide composition of the CS/DS is shown. Data presented as the mean ng GAG/ $\mu$ g DNA, for  $n = 4$ . Error bars are  $\pm$ SD,  $p$ -values are displayed. (C) Cell layers were also immunostained for HA, Vcan, Acan and Non-Immune IgG negative control. Scale bar: 30  $\mu$ m.

### Versican turnover in ADSCs and chondrocytes from WT, $ts5^{-/-P}$ and $ts5^{-/-J}$ mice

The previously reported requirement for TS5 in murine Vcan degradation [26–28] was examined for both ADSCs and chondrocytes from WT,  $ts5^{-/-P}$  and  $ts5^{-/-J}$  mice using three different antibodies. A typical set of blots with the three antibodies and a schematic of epitope locations are shown in Fig. 4. Western analyses with Ab1033 to the  $\beta$ -GAG domain (present in both Vcan V1 and V2) gave no evidence for TS5-dependent Vcan cleavage in ADSCs (Fig. 4A and S-2) since there were no major differences in band patterns between WT and both KO cultures. Further, antibody Vc [37] (Fig. 4B) detected two major products (at ~64 kDa and ~230 kDa) and these were also the same in all three genotypes of ADSCs. Some variability in total Vcan signal was seen and appeared to originate from culture variability, but it was not related to genotype. The major Ab1033-positive Vcan products in ADSC cultures from all genotypes were about 100 kDa (in cell layer) and 120 kDa (in medium) and two other major species, migrating at ~130 kDa and 150 kDa were present in both culture compartments (see Fig. 4D for all putative structures). A product >250 kDa, in the size range of full-length Vcan V2,

was detected in both ADSCs and chondrocytes (Fig. S-2) and it also showed variable abundance which was not related to genotype.

Analysis of chondrocyte products with Ab1033 (Fig. 4C) also showed no major differences between WT and  $ts5^{-/-P}$ , confirming that TS5 is also not required for proteolysis of Vcan in this differentiated cell type. The Vcan species between 75 kDa and 150 kDa (for all genotypes) required chondroitinase ABC digestion for maximum detection, consistent with some CS substitution of the  $\beta$ -GAG domain (Fig. 4D).

We next examined the possibility that aggrecanase-mediated cleavage of Vcan might be inhibited by the A2M in serum-containing cultures. We therefore attempted to promote proteolysis by placing cultures in 1% FBS. Western analysis of the cell-layers before serum deprivation (Fig. 5A, 0 h) showed some accumulation of the G1-DPE product (~60 kDa) in WT and both KO ADSCs. At 2 and 6 h culture in low serum, products secreted into the medium or present in the cell layers of ADSCs, were probed with  $\alpha$ -DPE (which detects the neoepitope formed on aggrecanase-mediated cleavage at 441E/A442). Consistent with the data in Fig. 4, there was no evidence for TS5-dependent generation of the neo-epitope in low serum, since the abundance of the G1-DPE product (~60 kDa) was

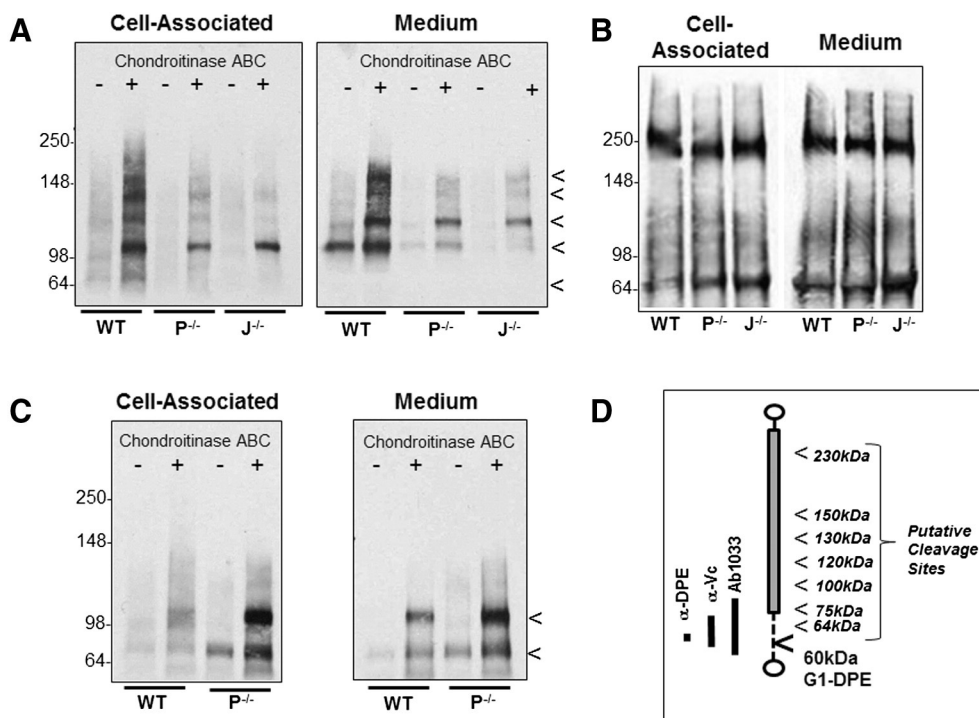


**Fig. 4.** Western analysis of Vcan from ADSCs and chondrocytes from WT and  $ts5^{-/-}$  mice maintained in 10% serum. (A) Ab1033 probe of cell-associated and media compartments from WT,  $ts5^{-/-P}$  ( $P^{-/-}$ ) and  $ts5^{-/-J}$  ( $J^{-/-}$ ) run  $\pm$  Chase ABC. (B) Anti-Vc probe of equivalent samples to (A) run with Chase ABC. (C) WT and  $ts5^{-/-P}$  chondrocyte cell-associated and media compartments, run  $\pm$  chondroitinase ABC. (D) Schematic representation of Vcan V2 with epitope locations and putative cleavage sites. Data presented is typical of 3 separate cell isolations for each cell type and genotype.

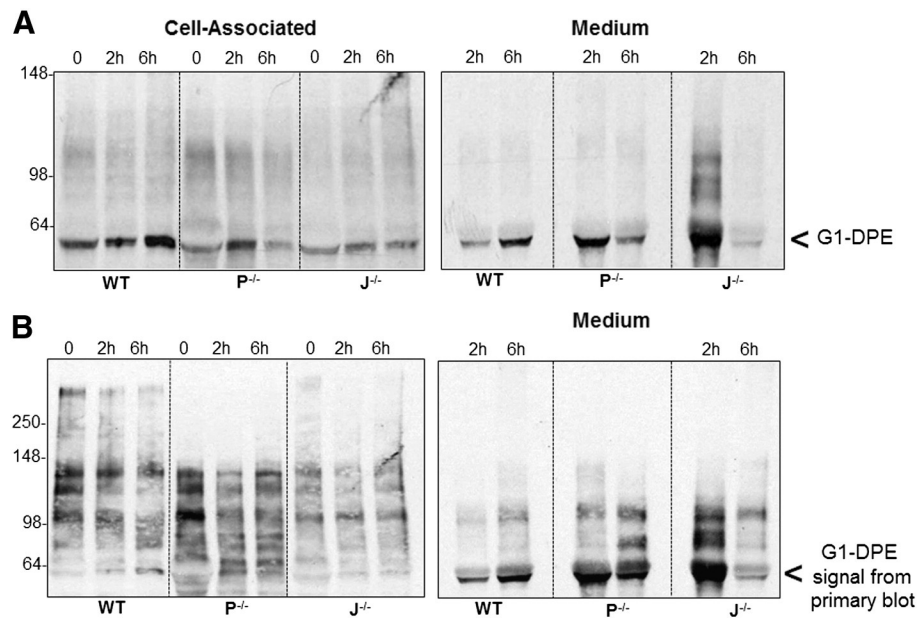


**Fig. 5.** Western analysis of Vcan catabolism in ADSC cultures changed to 1% serum. (A)  $\alpha$ -DPE probe of cell-associated products at 0, 2 and 6 h and media products at 2 and 6 h from WT,  $ts5^{-/-}P$  ( $P^{-/-}$ ) and  $ts5^{-/-}J$  ( $J^{-/-}$ ) ADSCs. (B) Ab1033 reprobe of membranes shown in (A). Note G1-DPE signal from (A) also detected in (B). Data presented is typical of 3 separate cell isolations for each cell type and genotype.

essentially the same at all times, in both WT and KO cultures (Fig. 5A). Confirmation was obtained by reprobing with Ab1033, since the products seen previously at about 75 kDa, 100 kDa, 120 kDa and 130 kDa (Fig. 5B) were again detected in WT and KO cultures. In summary, there was no evidence that elimination of TS5 prevented the formation of G1-DPE or any other truncated Vcan product. The fact that the same fragmentation occurs in 10% and 1% serum suggests that versicanolysis in WT and both  $ts5^{-/-}$  cells occurs in a location protected from serum inhibitors, and perhaps intracellularly.

#### Aggrecan turnover in ADSCs and chondrocyte cultures from WT, $ts5^{-/-}P$ and $ts5^{-/-}J$ mice

Similarly, the expected requirement for TS5 in Acan degradation [38,39] was examined by Western analysis of confluent ADSCs and chondrocytes from WT,  $ts5^{-/-}P$  and  $ts5^{-/-}J$  mice, and a typical set of blots is shown in Fig. 6. Analysis with  $\alpha$ -DLS (Fig. 6A), gave no evidence for TS5-mediated aggrecanolysis, since the species present in WT and both  $ts5^{-/-}$  ADSCs were similar, as was their distribution between medium and cell associated pool. All blots showed a broad band of DLS-reactive species, which on low exposure was resolved into bands of ~150 kDa, ~130 kDa, ~120 kDa (together labeled as species 2) and ~64 kDa (species 4) (see Fig. 6D for all putative core protein structures). For WT and both  $ts5^{-/-}$  ADSCs, cell-associated Acan core species were not

extensively substituted with CS (migration or abundance unaffected by chondroitinase digestion), however the 130 kDa and 150 kDa species secreted into the medium were highly substituted.

Portions of medium were further analyzed with antibodies to the aggrecanase neo-epitopes, SELE1480 and KEEE1667, and the calpain-generated neoepitope GVA (Fig. 6B). These results showed that species labeled as 1 (250 kDa), 2 (148 kDa) and 4 (64 kDa) are aggrecanase-generated fragments, and species 3 (100 kDa) is calpain generated (see Fig. 6D for all putative structures). This, in turn, shows that proteolysis of Acan at these sites occurs in the presence of 10% serum, and that again TS5 is not demonstrably involved. To support the identification of the Acan species in ADSCs, media and cell extracts were also prepared from chondrocytes for blotting with  $\alpha$ -DLS (Fig. 6C). The four major Acan species identified in ADSCs were also present in chondrocytes and again, no major differences were observed between WT and  $ts5^{-/-}P$  samples. It was noted that on a per cell basis, ADSCs produced about 30% of the Acan core and CS/DS made by chondrocytes in these cultures (data not shown). CS/DS substitution of Acan in chondrocyte samples was also examined by digestion with chondroitinase ABC (Fig. 6C) and, as observed for ADSCs, cell-associated core proteins were largely devoid of CS, whereas the medium contained the CS-substituted species. However, chondrocyte cultures contained a higher proportion of the CS-substituted 250 kDa species than ADSCs.

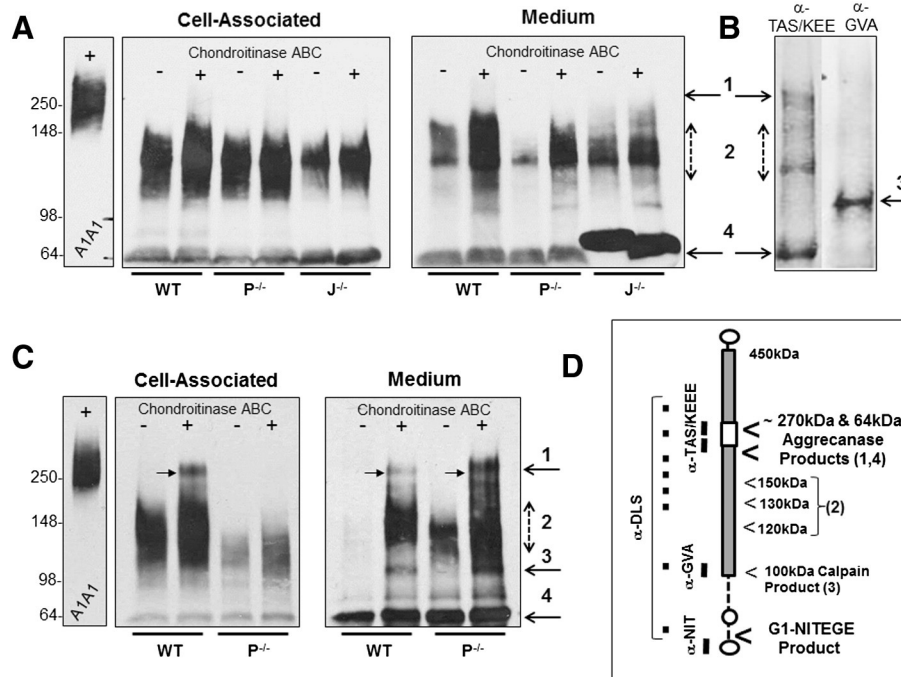


**Fig. 6.** Western analysis of Acan core proteins in ADSCs and chondrocytes from WT and *ts5*<sup>-/-</sup> mice maintained in 10% serum. (A) Proteoglycans from cell-associated and medium compartments of ADSCs from WT, *ts5*<sup>-/-</sup> P (*P*<sup>-/-</sup>) and *ts5*<sup>-/-</sup> J (*J*<sup>-/-</sup>) mice were probed with  $\alpha$ -DLS. (B) Portions of WT ADSC samples probed with a mixture of  $\alpha$ -TAS/ $\alpha$ -KEEE to detected CS-region aggrecanase neo-epitopes, and separately with  $\alpha$ -GVA to detect calpain-mediated Acan cleavage. (C) Proteoglycans from cell-associated and medium compartments of chondrocytes from WT and *ts5*<sup>-/-</sup> P mice were probed with  $\alpha$ -DLS. A1A1 lane is 10  $\mu$ g A1A1 human Acan. (D) Schematic representation of Acan with epitope locations and putative cleavage sites number-matched with immunoreactive bands. Note: By variable film exposure we estimated that 10% of the Acan and 50% of the Vcan were retained in the cell layer in cultures of this type. Data presented is typical of 3 separate cell isolations for each cell type and genotype.

We also assayed for potential enhancement of Acan proteolysis by placing cultures in 1% FBS. Western analysis of the cell-layers before serum deprivation (Fig. 7A, 0 h) showed some accumulation of the G1-NITEGE product (~60 kDa) in WT and both *ts5*<sup>-/-</sup> ADSCs. At 2 h and 6 h culture in low serum (Fig. 7A), similar amounts of a “dimeric” 120 kDa NITEGE-reactive species accumulated in cell layers of all three genotypes, but only minor amounts of this aggrecanase product were found in the culture media at either 2 or 6 h. These data also show that TS5 is not involved in the generation of any of the aggrecanase-generated Acan products. A reprobe of these membranes with  $\alpha$ -DLS confirmed the presence of species 1 and 2 (250 kDa and 150–120 kDa, respectively) in the cell layer of all genotypes at 0 h and showed that these species disappeared from the cell layer (Fig. 7B), as expected from the further generation of G1-NITEGE (Fig. 7A). Indeed, some of the expected DLS-reactive fragments were also detected in the medium (Fig. 7A and B).

The authenticity of the Acan degradation products in ADSCs (120 kDa–150 kDa ladder, Fig. 6D) was

supported by the presence of the same NITEGE-reactive products in chondrocyte cell layers (Fig. 7C). Furthermore, the “dimeric” form of G1-NITEGE product in ADSC cultures (Fig. 7A) was not due to aberrant glycosylation, since N-glycanase pre-treatment [40] did not alter the migration of the NITEGE positive band (Fig. 7D). It probably represents the same non-reducible “dimeric” form of G1-NITEGE described in human cartilage extracts [41]. We speculate that this species is formed by a protein cross-linking enzyme, such as a transglutaminase, in the aggrecan biosynthetic pathway of ADSCs and chondrocytes.

In summary, there was no evidence that TS5 is responsible for proteoglycan cleavage in ADSCs or chondrocytes, despite the fact that injuries to the dermis, diarthroidal joint and tendon, in *ts5*<sup>-/-</sup> P mice accumulate more aggrecan than WT [29,42,43].

#### ADSCs from *ts5*<sup>-/-</sup> mice take up glucose more rapidly than ADSCs from wild-types

Since there was no evidence that TS5 is responsible for proteoglycan cleavage in ADSCs or chondrocytes,

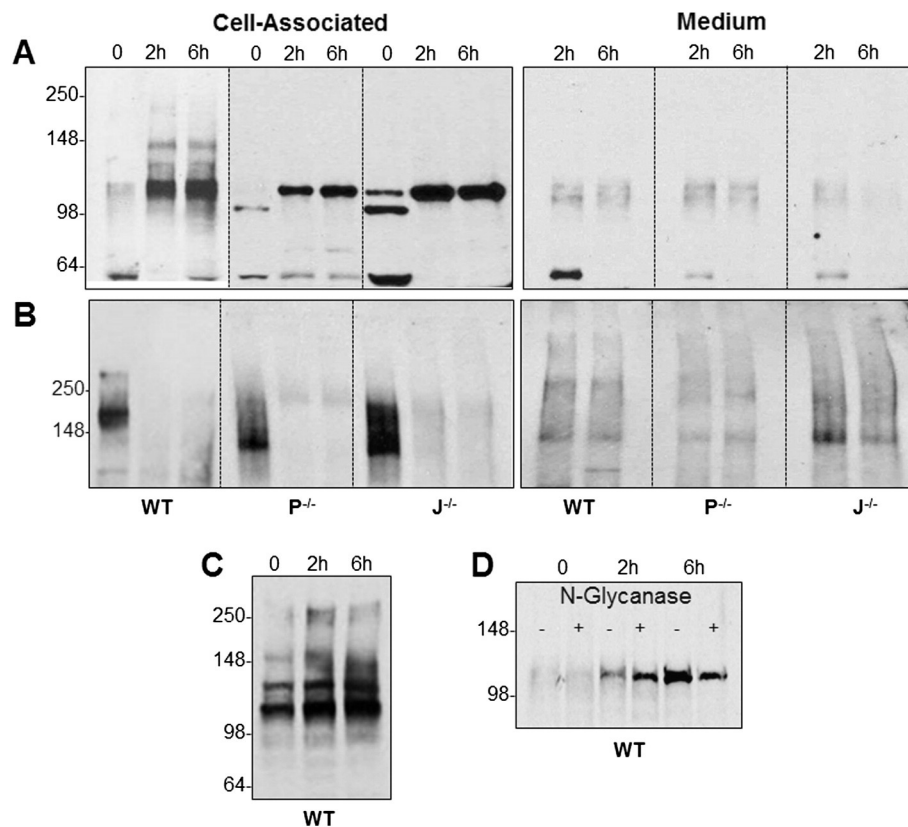


**Fig. 7.** Western analysis of Acan catabolism in ADSCs and chondrocytes from WT and *ts5*<sup>-/-</sup> mice changed to 1% serum. (A) Cell-associated and medium products from WT, *ts5*<sup>-/-</sup>P (*P*<sup>-/-</sup>) and *ts5*<sup>-/-</sup>J (*J*<sup>-/-</sup>) ADSCs probed with  $\alpha$ -NITEGE (B)  $\alpha$ -DLS re-probe of (A). (C) WT chondrocyte cell extracts probed with  $\alpha$ -NITEGE (D) Cell-associated WT ADSC samples treated  $\pm$  N-glycanase. Data presented is typical of 3 separate cell isolations for each cell type and genotype.

and yet dermal, diarthroidal joint and tendon injuries in *ts5*<sup>-/-</sup>P mice exhibit higher Acan expression and accumulate more hyalactans than WT [29,42,43], we speculated that the increases in *ts5*<sup>-/-</sup>P mice could result from a prolonged stimulated production of Acan and Vcan by MSCs in vivo. A potentially critical step in stimulating proteoglycan synthesis by MSCs is an enhanced glucose uptake through IGF-1 or insulin in MSC-mediated dermal healing [44] and in pro-chondrogenic responses of MSCs [45–47]. This mechanism would provide energy and UDP precursors for production of a provisional glycocalyx for survival of pluripotent cells in a wound, and prior to deposition of fibrous scar tissue. To test this, we examined glucose uptake in confluent WT and *ts5*<sup>-/-</sup>P ADSCs maintained for 4 h or 24 h in medium containing either 5 mM or 10 mM glucose. At both time points and at both glucose levels, the *ts5*<sup>-/-</sup>P cells took up markedly more glucose than WT cells (Fig. 8A), and a similarly elevated uptake was also seen over 24 h with *ts5*<sup>-/-</sup>J cells in 5 mM glucose (data not shown).

Since *ts5*<sup>-/-</sup>P ADSCs secreted markedly more HA than WT over 24 h (Fig. 3A, B), we decided to determine whether their higher consumption of

glucose also resulted in a higher production of CS-substituted aggrecan core. For this, we examined media and cell layers from cultures after the 24 h exposure to the two glucose concentrations. Western blot (typical blots shown Fig. 8B) confirmed that at both concentrations of glucose the *ts5*<sup>-/-</sup>P cells produced markedly more CS-substituted Acan (full-length, 1 and 2) than WT cells. Furthermore, glucose-induced CS substitution of Acan by ADSCs from both genotypes in 10 mM glucose was confirmed by Chase ABC digestion of the 24 h medium and cell fractions (Fig. 8C, top and bottom panels respectively). In contrast, Vcan production was not markedly affected by the increased glucose concentration or the deletion of TS5 (Fig. 8D) and this could be explained by different CS-addition pathways for Acan and Vcan.

#### LRP-1 is fragmented in WT but not *ts5*<sup>-/-</sup>P ADSCs

Since the absence of TS5 enhanced glucose uptake by ADSCs, we wondered whether this might be due to an increase in the glucose transporter

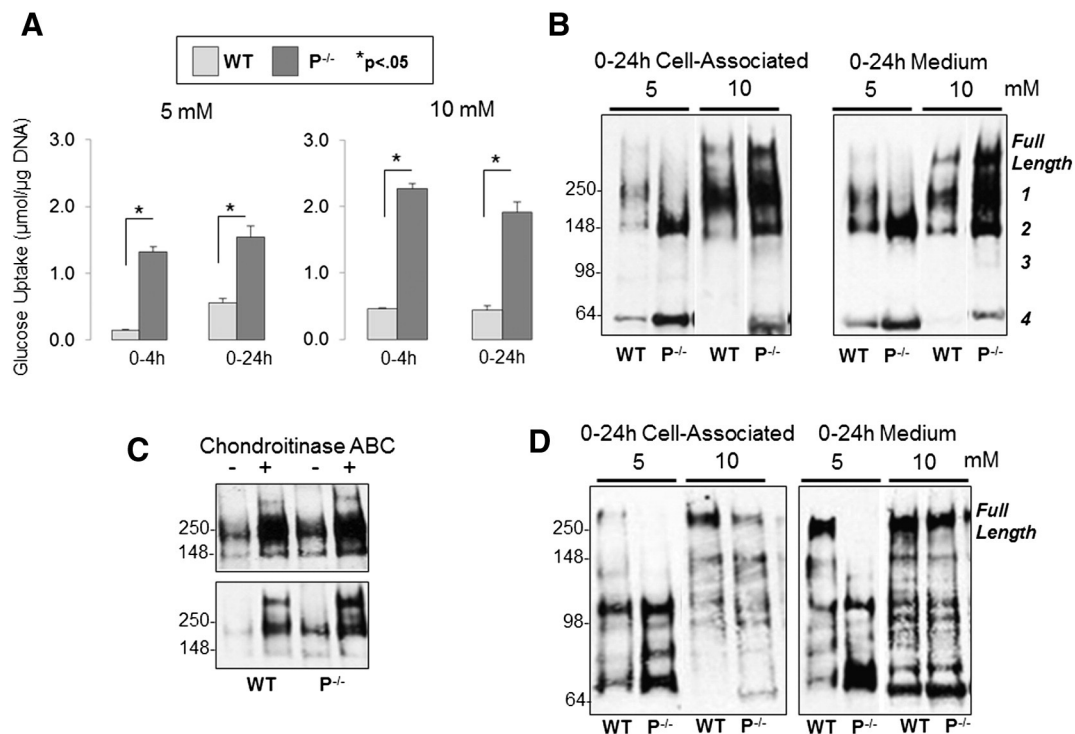


**Fig. 8.** Glucose uptake and proteoglycan synthesis by ADSCs from WT and *ts5*<sup>-/-</sup> mice. (A) Glucose uptake by ADSCs in medium containing 5 mM or 10 mM glucose. Glucose was measured in fresh medium and in medium collected after 4 h and 24 h. Uptake [Glc at 0 h–Glc at 4 h or 24 h] was calculated as μmol of glucose per μg DNA per 4 h or 24 h, (\**p* < 0.05, *n* = 4). (B) Western analysis (with α-DLS) of Acan in cell associated and medium samples after 24 h in 5 mM and 10 mM glucose (C) Effect of chondroitinase ABC digestion on Acan signal (α-DLS) of medium (above) and cell-associated products (below) in 10 mM glucose. (D) Western analysis of the same samples for Vcan with Ab1033.

GLUT4, however its mRNA abundance was very similar in the two genotypes and was not affected by culture conditions (data not shown). Since TS5 [48] and GLUT4 [49] are both known ligands of LRP-1, and LRP-1 is critically important for endocytotic recycling and translocation of GLUT4 to the cell surface, we next examined the abundance of transcripts and protein for LRP-1 in cultures treated for 4 h or 24 h in 5 mM or 10 mM glucose. The data showed that the abundance of LRP-1 mRNA was ~2-fold lower in untreated *ts5*<sup>-/-</sup> relative to WT ADSCs, and levels were even lower (~4-fold) in the KO cells after culture at both glucose concentrations (data not shown). However, Western analysis for the intact transmembrane 85 kDa β-chain [50] (Fig. 9A, lanes 1, 2 and Fig. 9B, upper panels) showed that its abundance was not markedly affected by genotype, but was increased in both genotypes in cultures maintained in 10 mM glucose (Fig. 9C). Higher exposure of the Western blot with the C-terminal-specific antibody (Fig. 9A, lane 3) revealed the presence of multiple lower mol. wt. species at ~60 kDa, 45 kDa, 35 kDa and 25 kDa, presumably generated by progressive N-terminal truncation of the intracellular domain of LRP-1 [51]. Whether this processing occurs while resident at the plasma membrane or within endocytotic vesicles

is currently unknown. Most notably, however, these truncated forms were absent or in very low abundance (relative to β-actin) in *ts5*<sup>-/-</sup> P cells (Fig. 9B & C). The lower β-actin signal in the *ts5*<sup>-/-</sup> P samples relative to WT shows that less cellular protein was loaded per volume of lysate. This is consistent with the finding that the typical DNA content of non-dividing ‘confluent’ culture of *ts5*<sup>-/-</sup> P ADSCs was ~50% of that measured for WT cultures, which is likely due to the greater degree of spreading and less dense packing of *ts5*<sup>-/-</sup> P cells on plastic as shown in Fig. 3. Taken together, these results indicate that a lack of TS5 in ADSCs reduces expression of LRP-1 and also impairs its intracellular proteolysis. Lastly, the gene expression of TS5 in WT cells was not markedly affected by the period of culture or concentration of glucose (not shown), and Western analysis of TS5 in these samples (Fig. 9D) showed that the abundance of the proteolytically “inactive” 38 kDa form (see Fig. 2) was also essentially unaffected.

## Discussion

We have presented data which provides a number of novel perspectives on the synthesis and

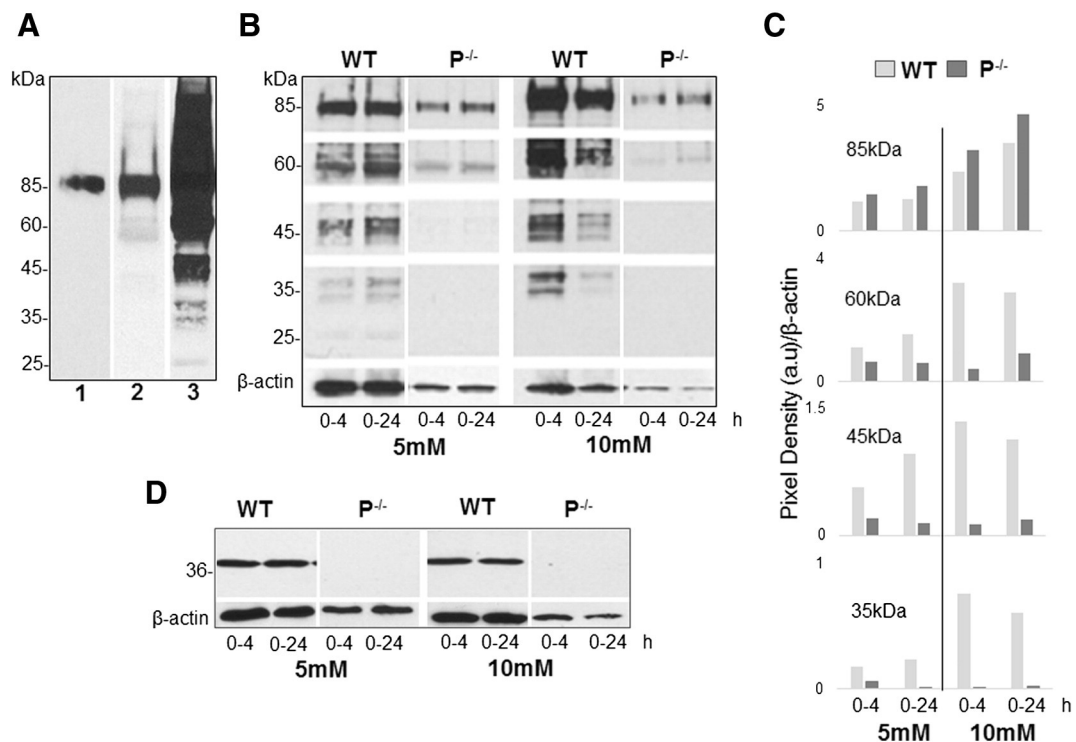


**Fig. 9.** LRP-1 and ADAMTS5 western analysis in ADSCs from WT and *ts5*<sup>-/-</sup> mice. (A) Lane 1: LRP-1 85 kDa transmembrane domain in extracts of murine spleen; lane 2, 85 kDa species in extracts from WT ADSC cells; lane 3, extended exposure times of Western blot from cell extracts showing the range of lower mol wt N-terminally truncated LRP-1 species. (B) anti LRP-1 Western of extracts from WT and *ts5*<sup>-/-</sup> P cells maintained for 4 or 24 h in medium containing 5 mM or 10 mM glucose, and blots exposed for 1 and 5 min to visualize the 85 kDa or truncated products, respectively. (C) Membranes were reprobbed with anti-β-actin, band intensities determined using ImageJ and abundance of LRP-1 species calculated relative to β-actin. (D) anti-TS5 (α-cat) Western of extracts from WT and *ts5*<sup>-/-</sup> P cells maintained for 4 or 24 h in medium containing 5 mM or 10 mM glucose.

degradation of Acan and Vcan in connective tissue cells, and in particular a new and apparently non-proteolytic role for TS5 in this process. There has been much debate over the role of TS5 in murine and human tissues; for example it was shown previously [38] that the Acan degradation product (G1-NITEGE) could not be detected in cartilage extracts from *ts5*<sup>-/-</sup> mice suggesting that TS5 activity must be responsible for cartilage Acan degradation. These findings were re-enforced by the finding that TS5 ablation prevented the formation of the equivalent Vcan product (G1-DPEAAE) in atherosclerosis [52], aortic valve disease [53], myxomatous valve disease [27] interdigital web regression [54] and myofibroblast differentiation [26]. While these data suggested that TS5 was responsible, there are at least two possible alternative explanations for the findings. For example, TS5 ablation might result in activation of other proteases which degrade G1-NITEGE and G1-DPEAAE, or TS5 ablation might promote endocytotic clearance of the G1 species, a process which has previously been demonstrated for G1-NITEGE with cells in vitro [55].

Studies in the present paper (Figs. 5, 7 and 8) show clearly that TS5 is not required for aggrecanase-mediated cleavage of Acan or Vcan with isolated ADSCs or chondrocytes from either *ts5*<sup>-/-</sup> P mice (used primarily to study Acan cleavage [30,42,56]) or *ts5*<sup>-/-</sup> J mice (used to study Vcan cleavage [52–54]). It should be noted that this is not an observation restricted to isolated cells since a number of reports from in vivo studies directly support this conclusion. Thus, IHC of growth plate cartilage in *ts5*<sup>-/-</sup> mice shows robust G1-NITEGE staining [39] and joint extracts from *ts5*<sup>-/-</sup> mice contain aggrecanase-generated cleavage fragments in abundance [42]. Moreover, cartilage explants from *ts5*<sup>-/-</sup> mice release aggrecanase-generated products [57,58], and TS5 is not required for the aggrecanase-generated products of Acan in the injured spine [59], nor is it essential for Vcan cleavage in stage E13.5 mouse embryos [31].

A conclusion that TS5 is not required for cleavage of aggrecan or versican, necessitates that one or more of the other aggrecanases (TS1, 4, 8, 9, 15) is active in *ts5*<sup>-/-</sup> mice. However, finding that TS5 is not required does not prove that TS5 is not responsible for aggrecanase activity in WT mice. The notion that

TS5 is not responsible is supported by the finding that TS5 protein in WT mouse muscle extracts and in WT ADSCs is present in forms at or below ~40 kDa (Fig. 2), all of which have been shown to be essentially inactive against Acan as a substrate [32]. The significance of the inactive ~40 kDa species described here (Fig. 2) is that it appears to represent a major natural form of TS5, most evident when extracts of fresh tissues, such as larynx [60], cartilage [61] and tendon [62] are analyzed. In addition there is a well-characterized ~50 kDa form in human synovial fluids [63]. The proteinase(s) responsible for these C-terminally truncated forms is unknown, but their size indicates that they could represent auto-proteolytic products, formed in vivo by TS5 cleavage at the known E753/G754 site [64] and a putative D642/A643 site, respectively. Indeed the sequence at the D642/A643 site is highly suited to aggrecanase-mediated cleavage, and since TS5 is the only aggrecanase which contains this sequence, it may play a unique role in TS5, such as a capacity for rapid inactivation of catalytic properties. Taken together with the published studies on this topic we have interpreted our new data to mean that TS9 is non-redundantly responsible for both Acan and Vcan cleavage in progenitor and differentiated cells in the mouse. The major unexpected finding supporting this conclusion is that the aggrecanase responsible must be active intracellularly. Such an intracellular location is supported by the following findings: a) The proteolytic activity was not affected by the potent inhibitory effects of serum A2M and b) the degradation products were solubilized from the cell layer by addition of 10× PIs and a short term extraction in denaturing 7 M urea, 50 mM TrisAcetate, and pH 8.0. These products were not however solubilized by treatment of cell layers with Strep-Hyase in PBS as described [29] c) both cell layers and medium contained aggrecanase-cleaved Acan products (as shown by the neo-epitope positive species 1, 2, 4 in the medium (Fig. 6) and G1-NITEGE in the cell layer (Fig. 7); d) both cell layers and medium from ADSCs contained aggrecanase-cleaved versican products, as shown by the presence of the G1-DPEAAE fragment in all samples (Fig. 5). e) The ADSC cell layer Acan products were not substituted with CS (unaffected by Chase ABC digestion) (Fig. 6A, left panel) whereas the medium products were substituted (altered by Chase ABC digestion) (Fig. 6A, right panel) and the same observations were made with chondrocytes (Fig. 6C). This finding of aggrecanase-cleaved non-substituted core is perhaps the strongest evidence for intracellular cleavage of both Acan and Vcan in both cell types because it places aggrecanase-mediated proteolysis upstream of CS-substitution and sulfation, which occurs in the late Golgi, immediately before secretion. The presence of CS-substituted species in the medium (Figs. 4A & C, 6A & C) confirms that CS synthesis was fully competent in these cells, and that the

generation of un-substituted cleaved forms was not a result of the absence of the necessary CS synthesizing enzymes.

Such proteolysis during secretion is also supported by the presence of a long-lived biosynthetic pool of precursor Acan in a specialized ER compartment of chondrocytes [65] and the intense staining of chondrocyte membranes with neoepitope antibodies to fragmented Acan [61] and Vcan [28]. It is also consistent with the papers that show aggrecanase-generated neo-epitopes in close association with cells, where the substrate pool of extracellular proteoglycan is comparatively limited, such as prostate stromal cells [66], myoblasts [28], adipocytes [24], neurons [67,68] fibroblasts [69], myofibroblasts [38], BMSCs [70] and glioblastomas [71]. Taken together, these data suggest that the concentration of Acan and Vcan in tissues is not primarily controlled by proteolysis in the ECM but by degradation during secretion, a mechanism with obvious control advantages for cells. In addition the proteolysis appears to occur very late in biosynthesis (before, during or after CS addition) since most of the degraded Vcan (Fig. 4), and some of the degraded Acan (Fig. 6) is CS-substituted. These findings also pose the important question of which clan member is, in fact, non-redundantly responsible for intracellular Acan and Vcan degradation. It is unlikely that TS5 or TS15 are involved because they are activated only after secretion [72,73], whereas TS1 and TS4 can be excluded because their null-mice generate the same aggrecanase products as the WT [74]. TS8 is an unlikely candidate due to its extremely low aggrecanase activity [75], and its established post-secretory role as an anti-angiogenic factor [76]. Therefore, when taken together, the available information suggests that TS9 is the aggrecanase primarily responsible for in vivo cleavage of hyalactans. This conclusion could explain why TS9-null mice die at E7.5 [77], since robust hyalactan turnover is presumably essential for skeletal development [78]. Also, TS9 appears ideally suited to the intracellular proteolysis described here, since the pro-form is active inside the cell and is inactivated by furin just before secretion [79,80]. Moreover, knockdown of chondrocyte TS5 or TS9 promotes matrix deposition [81] and interestingly, TS9 is the most evolutionarily conserved clade member, consistent with a central and non-redundant function [82].

It is recognized that this hypothesis does not exclude a role for other aggrecanases, such as TS4 and TS5 in cartilage explant systems, however it is conceivable that some of the subtle control mechanisms of matrix turnover which operate in vivo are partially lost on explant culture with stimulatory cytokines.

The data presented here and elsewhere indicate that accumulation of Acan at wound sites in *ts5*<sup>-/-</sup>

mice is not due to an absence of its removal by TS5, but rather, the result of a marked stimulation of its synthesis and deposition due to an amplified uptake of glucose by local reparative cells. This seems reasonable since Acan production requires a high level of CS synthesis, which is dependent on the intracellular supply of glucose for UDP-N-acetylgalactosamine and UDP-glucuronic acid precursors. A potential explanation for how an absence of TS5 could enhance glucose uptake is provided by findings that the abundance of both TS5 [48] and GLUT4 [49,83] at the cell surface is reduced by their endocytosis in association with a common receptor, LRP-1. The capacity of LRP-1 to bind and endocytose ligands such as MMPs has been shown to be down-regulated by MT1-MMP-mediated cleavage and loss of the ligand-binding  $\alpha$ -chain while leaving the 85 kDa  $\beta$ -chain intact [50]. Our analyses of LRP-1 protein in ADSCs using a C-terminal specific antibody, was confined to detection of the  $\beta$ -chain. We detected N-terminally cleaved forms of the  $\beta$ -chain, and such processing could provide an additional mechanism for down-regulating ligand binding and/or endocytosis or simply be the result of endosomal proteolysis following translocation of the LRP-1 with its ligands into such intracellular compartments. Notably, the abundance of these truncated forms was markedly lower in *ts5*<sup>-/-</sup>P cell extracts, suggesting that binding of ligands, such as GLUT4 and their endocytosis is reduced in the absence of TS5. What effect this might have on the abundance of the GLUT4 pool provided to the membrane in GLUT storage vesicles, and actively involved in glucose uptake, remains to be determined. Whatever the precise mechanism by which TS5 depresses glucose uptake, the data are consistent with it having a non-proteolytic role in controlling the cell surface interaction between GLUT4 and LRP-1, and thereby in modulating the energy status of cells. Further examination of the dynamics of endocytotic pathways in wild type and *ts5*<sup>-/-</sup> cells, at the biochemical and ultrastructural levels, offers an opportunity to delineate the dynamics of the relationship between membrane transporters and cellular rates of glucose uptake during tissue regeneration.

Finally, the functional significance of Acan production by undifferentiated stromal cells and fibroblasts is unclear, since it is not stably incorporated as a proteoglycan into their extracellular matrix. However, taken together with the known accumulation of an intracellular Acan core protein pool (Fig. 3C [84,85]), CS-Acan secretion could serve to stabilize intracellular ATP levels by utilizing an excess of high-energy sugar substrates, formed, for example, after rapid glucose uptake by cells in a wound [86]. Indeed a similar mechanism for reducing cell stress has been reported for the enhanced HA secretion [87–89] that occurs under hyperglycemic conditions.

Moreover, these findings need to be taken into consideration when interpreting 'chondrogenic' differentiation responses in pluripotent cells, which are often done in media with supra-physiologic concentrations of glucose. Thus, assays of sulfated GAG accumulation may be misleading, because such accumulation might occur as a stress response to glucose in fresh medium and result in the deposition of a 'pro-inflammatory' matrix [90], which would diminish functionality of such material for cartilage implantation. A detailed biochemical and structural analyses of progenitor cell-generated tissues *in vivo* and *in vitro* [91] therefore remains essential.

## Materials and methods

### Mouse strains

All mouse breeding and experimental procedure were carried out under approved IACUC protocols. The two TS5 knockout strains used in this study, *ts5*<sup>-/-</sup> (Lexicon) (denoted *ts5*<sup>-/-</sup>P) and *ts5*<sup>-/-</sup> (Jackson) (denoted *ts5*<sup>-/-</sup>J), both with deletion of exon 2, have been described [27,30]. Both KO strains were backcrossed six times into the in house maintained wild type C57Bl/6 strain. Genomic DNA and mRNA preparation and agarose electrophoresis used standard protocols, and PCR was performed with the following primer sets: For *ts5*<sup>-/-</sup>P: forward 5'-TTTGAATTTGTCTTTGGAAGGCCTC-3', reverse 5'-GACAGTGTGACTCATCCGGGATA-3'; for *ts5*<sup>-/-</sup>J: forward 5'-GCATACCACTCCAACTTAGAGAGG-3', mutant-neo 5'-GGGCCAGCT-CATTCCTCCCACTCAT-3' and reverse 5'-CGCAGCTGACTGCTCTTGTGCTTG-3'.

mRNA was isolated from WT and *ts5*<sup>-/-</sup> ADSCs, using the RNeasy kit (Qiagen) and cDNA prepared with the iScript kit (Bio-Rad) and QPCR amplification was done with the following primers. Primer set 'I' (Fig. 1B, F); 5'-GAGCACTACGATGCAGCCAT-3', and 5'-CACAGACATCCATGCCAGGG-3'. Primer set 'II' (Fig. 1C, F); 5'-TGTTACCCGAGAGGGCATC-3' and, 5'-TGTC AAGTTGCACTGCTGGG-3'. Primer set 'III' (Fig. 1C, G); 5'-AGCAAGCATCCAGCTAGACTCA-3' and 5'-TTTGTGCATTAGAGTAAACCACAGG-3'. For sequence analyses of amplified PCR fragments they were purified using QIAquick PCR purification columns (Qiagen) and cloned into pDrive plasmid vector (Qiagen). Five recombinant clones from each genotype were sequenced and compared to each other using ClustalW2 alignment (EMBL-EBI).

### Western blot analysis of TS5 protein

Gastrocnemius muscle (~100 mg) was harvested immediately after sacrifice, washed in cold PBS containing proteinase inhibitors (Roche Complete

Mini), rinsed and snap frozen in liquid N<sub>2</sub> before being powdered in a Bessman pulverizer. Powder was extracted in 300  $\mu$ L Laemmli sample buffer (BioRad) with proteinase inhibitors at 100 °C for 10 min with mixing. Also, confluent ADSCs were extracted in 100  $\mu$ L 50 mM Tris HCl pH 7.5, 150 mM sodium chloride, 5 mM EDTA, 1% NP-40, 10 mM sodium fluoride, 100 mM sodium orthovanadate and proteinase inhibitors for 15 min at 4 °C with mixing, and 2  $\mu$ L of the serum batches used in this study (Atlanta Biologics, E1101, B12027, H12120, A13005) were mixed with 98  $\mu$ L of Laemmli sample buffer (plus proteinase inhibitors) and heated at 100 °C for 10 min. Insolubles were removed by centrifugation and 10  $\mu$ L (equivalent to about 3 mg of muscle), 5  $\mu$ L (corresponding to products of  $\sim 2 \times 10^4$  cells) and 10  $\mu$ L (equivalent to 0.2  $\mu$ L of serum) were run on 4–12% SDS PAGE and analyzed by Western with antibodies against residues 338–368 of the catalytic domain ( $\alpha$ -cat, Ab135656, 0.25  $\mu$ g/mL, Abcam) and residues 636–649 of the Cys-rich region ( $\alpha$ -cys, KNG [61] at 2  $\mu$ g/mL).

### Isolation and culture of murine ADSCs and epiphyseal chondrocytes

ADSC cultures were prepared from abdominal and groin adipose essentially as described in [92]. Briefly, for each separate experiment, tissue was harvested from five 10–12 week male mice into CO<sub>2</sub>-independent medium (Gibco) and dispersed under agitation for 2 h at 37 °C in 25 mL of CO<sub>2</sub>-independent medium with 3 mg/ml collagenase type II (Worthington). The digest was centrifuged at 300  $g$  for 10 min, the lipid-rich layer discarded, the pellet treated with 1.5 mL RBC lysis buffer (eBioscience) and then washed three times in PBS, before suspension in 30 mL DMEM/5 mM glucose/10% FBS containing 2 ng/mL bFGF and plating in a T75 flask. Non-adherent cells were removed after 24 h and fresh medium was added. Medium changes were performed every 48–72 h. Cells were expanded at  $\sim 90\%$  confluence by trypsinization (1:3 split) and used in T25 flasks after 2 passages. Typical cell morphologies at each passage are shown in Fig. S-1A, B.

For primary chondrocyte cultures, cartilages were collected from the epiphyses of the tibia and femur of six one-week old mice, into CO<sub>2</sub>-independent medium. Digestion was as described [93] and cells were plated in 60 mm dishes at  $7 \times 10^4$  cells/cm<sup>2</sup> and maintained in Advanced MEM, 5 mM glucose, 10% FBS. Medium was changed daily, confluence was reached by day 4, and typical cell morphology is shown in Fig. S-1C.

### QPCR assay for gene expression

Total RNA was purified from confluent ADSCs and chondrocytes with TRIzol® using the Ambion

protocol. The RNA pellet was suspended in 100  $\mu$ L RNase/DNase free water (Gibco) and further purified using the RNeasy kit (Qiagen). RNA purity and yield were determined, mean yield for  $\sim 3 \times 10^6$  cells was  $1290 \pm 725$  ng/ $\mu$ L, and mean 260 nm/280 nm ratio was  $2.08 \pm 0.013$ . cDNA was synthesized from 1  $\mu$ g RNA with the First-Strand Synthesis Kit (Invitrogen), then diluted 10-fold and combined with Taqman™ Gene Expression Master Mix (Applied Biosystem, Inc.). QPCR was done using the Taqman™ platform (Life Technologies), and primers used in this study are given in Table S-1. Data are presented as mRNA abundance relative to *Gapdh*, calculated as  $(2^{-\Delta C_t}) \times 1000$  (arbitrary units).

### Acan and Vcan purification and Western analysis in ADSC and chondrocyte cultures

At confluence, cultures were changed into fresh medium (for ADSCs, DMEM:AMEM (3:1)/5 mM glucose plus 10% FBS; for chondrocytes, AMEM/5 mM glucose/plus 10% FBS). For termination, cultures were placed on ice, medium was removed and adjusted to 7 M urea including proteinase inhibitors. Cell layers were solubilized by sequential addition of 300  $\mu$ L of a 10 $\times$  protease inhibitor solution (150 mM benzamide, 50 mM EDTA, 1 mM AEBSF, 50 mM IAA, 5  $\mu$ g/mL pepstatin and 10  $\mu$ g/mL leupeptin, Sigma Aldrich) and 3 mL 7 M urea, 50 mM TrisAcetate, pH 8.0, and clarified by centrifugation (14,000  $g$  for 5 min). Media and cell extracts were fractionated by anion exchange chromatography using DE52 resins as described [29], and purified proteoglycans were separated on 4–12% gradient gels, before and after treatment with chondroitinase ABC, and then visualized by Western blot. For ADSCs and chondrocyte products, each lane was loaded with medium or cell extract from  $\sim 2 \times 10^6$  cells. Western analysis of Acan was done with  $\alpha$ -DLS [29],  $\alpha$ -NITEGE and  $\alpha$ -TASELE/TFKEEE [42] and  $\alpha$ -GVA [94], all at 1  $\mu$ g/mL. For Vcan, Ab1033 (Abcam) was used at 1:1000,  $\alpha$ -DPEAAAE [95] at 1  $\mu$ g/mL and anti-Vc [37] at 1:1000 (anti-Vc was a kind gift from Dr. Simon Foulcer). As previously reported for fibroblasts [29]  $>90\%$  of the Vcan and Acan species recovered from ADSC and chondrocyte cultures, including the non-CS-substituted G1-products, were recovered in the DE52-bound fraction (data not shown). Data shown is typical of 3 separate cell isolations for each cell type and genotype.

### Glucose uptake and Western blot analysis of LRP1 and ADAMTS5 in ADSC cultures

Cultures of WT and *ts5*<sup>-/-</sup>P ADSCs were established after the 2nd passage by plating  $\sim 0.5 \times 10^6$  cells per well in 12-well plates maintained in 1 mL DMEM/5 mM glucose/10% FBS/2 ng/mL bFGF for

24 h, and for an additional 24 h in DMEM:AMEM (3:1), 5 mM glucose/10% FBS, after which DNA contents of cultures remained unchanged. Media were changed to DMEM:AMEM (3:1)/10% FBS containing 5 or 10 mM glucose. Medium was removed at 4 h or 24 h and assayed for glucose content using the Amplex™ kit (LifeTech Inc.). Briefly, 0.1 µL media (serially diluted from 10 µL portion) was measured in a total reaction volume of 100 µL. Uptake data were calculated from the change in medium glucose concentration, and expressed as µmol of glucose per µg DNA per 4 h or 24 h. For LRP-1 and ADAMTS5 Western analyses, 4 h and 24 h treated cell layers were solubilized for 15 min at 4 °C in 100 µL 50 mM Tris HCl pH 7.5, 150 mM sodium chloride, 5 mM EDTA, 1% NP-40, 10 mM sodium fluoride, 100 mM sodium orthovanadate and proteinase inhibitors, insolubles were removed by centrifugation. 10 µL portions were mixed with 20 µL of Laemmli sample buffer (plus proteinase inhibitors), heated at 100 °C for 10 min and were run on 4–12% SDS-PAGE gels, Western analyses performed using anti-LRP-1 (ab92544, Abcam, 200 µg/mL) and anti-TS5 (α-cat Ab135656, Abcam, 0.25 µg/mL).

### Other methods

HA and CS/DS content of ADSC cultures was determined by fluorophore-assisted carbohydrate electrophoresis (FACE) as described [96]. DNA was assayed in proteinase K-digested cell layers with Hoechst 33258 as described [97]. Typical DNA contents of non-dividing 'confluent' culture of *ts5<sup>-/-</sup>* ADSCs was ~50% of that measured for WT cultures. The lower cell density in non-dividing KO cultures is likely due to the greater degree of spreading and less dense packing of these cells on the plastic.

### Immunohistochemistry for HA, aggrecan and versican

ADSCs were grown to ~90% confluence in 8-well chamber slides (Nunc™ Lab-Tek™ II) and maintained for 24 h in DMEM:AMEM (3:1), 5 mM glucose plus 10% FBS. The medium was removed and cell layers rinsed twice with PBS before fixation in Histochoice™ (Amresco). HA was visualized with biotinylated HABP at 1 µg/mL [98,99], Acan with α-DLS and Vcan with Ab1033, and counterstained with Methyl Green. *S. hyaluronidase* treatments were done as described [29] and 1 µg/mL non-immune rabbit IgG was used as the negative control.

### Statistical methods

Group differences (mean ± SD) were evaluated with Students t-test and p-values are shown. For QPCR analyses n = 6 (3 replicates from 2 separate experiments), glucose uptake assay n = 4 (4 replicates

from 1 experiment) and FACE n = 4 (4 replicates from 1 experiment).

Supplementary data to this article can be found online at <http://dx.doi.org/10.1016/j.matbio.2015.03.008>.

### Acknowledgments

We gratefully acknowledge Dr. Simon Foulcer for making the anti-Vcan (Vc) antibody available and Dr. Tibor Rauch for his assistance in the analyses of *ts5<sup>-/-</sup>* gene modifications and mRNA transcripts sequencing and Dr. Vincent Hascall for discussions throughout the study.

Funding for authors include The Katz-Rubschlager Endowment for OA Research (AP, DJG); NIH R01-AR057066 from NIAMS (DJG, AP, WX, JL, JDS) and P01HL107147 from NHLBI (ML). The content is solely the responsibility of the authors and does not necessarily represent the official views of NIAMS and NHLBI.

Received 23 December 2014;

Received in revised form 25 March 2015;

Accepted 26 March 2015

Available online xxx

### Keywords:

ADAMTS5 knock out;

ADAMTS5;

Aggrecan;

Versican;

Hyaluronan;

Degradation;

Adipose derived stromal cells;

Mesenchymal stem cells

### Abbreviations used:

A2M, alpha-2-macroglobulin; ADSC, adipose derived stromal cell; Acan, aggrecan; Vcan, versican; CS/DS, chondroitin/dermatan sulfate; DE52, diethyl-amino-ethyl cellulose; ECM, extracellular matrix; HA, hyaluronan; IHC, immunohistochemistry; KO, knockout; LRP1, lipoprotein receptor related protein-1; TGF-β1, transforming growth factor beta-1; BMP7, bone morphogenetic protein 7; TS5, a disintegrin and metalloproteinase with thrombospondin motifs 5; *ts5<sup>-/-</sup>*-J, TS5 knockout mouse from Jackson Labs; *ts5<sup>-/-</sup>*-P, TS5 knockout mouse from Lexicon; WT, wild type.

### References

- [1] Kretzschmar K, Watt FM. Markers of epidermal stem cell subpopulations in adult mammalian skin. *Cold Spring Harb Perspect Med* 2014;4.

- [2] da Silva Meirelles L, Chagastelles PC, Nardi NB. Mesenchymal stem cells reside in virtually all post-natal organs and tissues. *J Cell Sci* 2006;119:2204–13.
- [3] Zuk PA, Zhu M, Mizuno H, Huang J, Futrell JW, Katz AJ, et al. Multilineage cells from human adipose tissue: implications for cell-based therapies. *Tissue Eng* 2001;7:211–28.
- [4] Maxson S, Lopez EA, Yoo D, Danilkovitch-Miagkova A, Leroux MA. Concise review: role of mesenchymal stem cells in wound repair. *Stem Cells Transl Med* 2012;1:142–9.
- [5] Sharma RR, Pollock K, Hubel A, McKenna D. Mesenchymal stem or stromal cells: a review of clinical applications and manufacturing practices. *Transfusion* 2014;54:1418–37.
- [6] Lindroos B, Suuronen R, Miettinen S. The potential of adipose stem cells in regenerative medicine. *Stem Cell Rev* 2011;7:269–91.
- [7] Lim MH, Ong WK, Sugii S. The current landscape of adipose-derived stem cells in clinical applications. *Expert Rev Mol Med* 2014;16:e8.
- [8] Cordeiro-Spinetti E, de Mello W, Trindade LS, Taub DD, Taichman RS, Balduino A. Human bone marrow mesenchymal progenitors: perspectives on an optimized in vitro manipulation. *Front Cell Dev Biol* 2014;2:7.
- [9] Lund TC, Boitano AE, Delaney CS, Shpall EJ, Wagner JE. Advances in umbilical cord blood manipulation—from niche to bedside. *Nat Rev Clin Oncol* 2014;12(3):163–74.
- [10] Lv FJ, Tuan RS, Cheung KM, Leung VY. Concise review: the surface markers and identity of human mesenchymal stem cells. *Stem Cells* 2014;32:1408–19.
- [11] Chen XD. Extracellular matrix provides an optimal niche for the maintenance and propagation of mesenchymal stem cells. *Birth Defects Res C Embryo Today* 2010;90:45–54.
- [12] Rezza A, Sennett R, Rendl M. Adult stem cell niches: cellular and molecular components. *Curr Top Dev Biol* 2014;107:333–72.
- [13] Klamer S, Voermans C. The role of novel and known extracellular matrix and adhesion molecules in the homeostatic and regenerative bone marrow microenvironment. *Cell Adhes Migr* 2014;8:563–77.
- [14] Coulson-Thomas VJ, Gesteira TF, Hascall V, Kao W. Umbilical cord mesenchymal stem cells suppress host rejection: the role of the glycocalyx. *J Biol Chem* 2014;289:23465–81.
- [15] Boivin WA, Shackelford M, Vanden Hoek A, Zhao H, Hackett TL, Knight DA, et al. Granzyme B cleaves decorin, biglycan and soluble betaglycan, releasing active transforming growth factor-beta1. *PLoS ONE* 2012;7 [Epub 2012 Mar 30].
- [16] Ning L, Kurihara H, de Vega S, Ichikawa-Tomikawa N, Xu Z, Nonaka R, et al. Laminin alpha1 regulates age-related mesangial cell proliferation and mesangial matrix accumulation through the TGF-beta pathway. *Am J Pathol* 2014;184:1683–94.
- [17] Nurcombe V, Cool SM. Heparan sulfate control of proliferation and differentiation in the stem cell niche. *Crit Rev Eukaryot Gene Expr* 2007;17:159–71.
- [18] Knelson EH, Gaviglio AL, Nee JC, Starr MD, Nixon AB, Marcus SG, et al. Stromal heparan sulfate differentiates neuroblasts to suppress neuroblastoma growth. *J Clin Invest* 2014;124:3016–31.
- [19] Qu C, Rilla K, Tammi R, Tammi M, Kroger H, Lammi MJ. Extensive CD44-dependent hyaluronan coats on human bone marrow-derived mesenchymal stem cells produced by hyaluronan synthases HAS1, HAS2 and HAS3. *Int J Biochem Cell Biol* 2014;48:45–54.
- [20] Midgley AC, Rogers M, Hallett MB, Clayton A, Bowen T, Phillips AO, et al. Transforming growth factor-beta1 (TGF-beta1)-stimulated fibroblast to myofibroblast differentiation is mediated by hyaluronan (HA)-facilitated epidermal growth factor receptor (EGFR) and CD44 co-localization in lipid rafts. *J Biol Chem* 2013;288:14824–38.
- [21] Lynch K, Pei M. Age associated communication between cells and matrix: a potential impact on stem cell-based tissue regeneration strategies. *Organogenesis* 2014;10:289–98.
- [22] Rocha B, Calamia V, Casas V, Carrascal M, Blanco FJ, Ruiz-Romero C. Secretome analysis of human mesenchymal stem cells undergoing chondrogenic differentiation. *J Proteome Res* 2014;13:1045–54.
- [23] Schlotzer-Schrehardt U, Dietrich T, Saito K, Sorokin L, Sasaki T, Paulsson M, et al. Characterization of extracellular matrix components in the limbal epithelial stem cell compartment. *Exp Eye Res* 2007;85:845–60.
- [24] Voros G, Sandy JD, Collen D, Lijnen HR. Expression of aggrecan(ases) during murine preadipocyte differentiation and adipose tissue development. *Biochim Biophys Acta* 2006;1760:1837–44.
- [25] Mariman EC, Wang P. Adipocyte extracellular matrix composition, dynamics and role in obesity. *Cell Mol Life Sci* 2010;67:1277–92.
- [26] Hattori N, Carrino DA, Lauer ME, Vasanji A, Wylie JD, Nelson CM, et al. Pericellular versican regulates the fibroblast-myofibroblast transition: a role for ADAMTS5 protease-mediated proteolysis. *J Biol Chem* 2011;286:34298–310.
- [27] Dupuis LE, McCulloch DR, McGarity JD, Bahan A, Wessels A, Weber D, et al. Altered versican cleavage in ADAMTS5 deficient mice; a novel etiology of myxomatous valve disease. *Dev Biol* 2011;357:152–64.
- [28] Stupka N, Kintakas C, White JD, Fraser FW, Hanciu M, Aramaki-Hattori N, et al. Versican processing by a disintegrin-like and metalloproteinase domain with thrombospondin-1 repeats proteinases-5 and -15 facilitates myoblast fusion. *J Biol Chem* 2013;288:1907–17.
- [29] Velasco J, Li J, DiPietro L, Stepp MA, Sandy JD, Plaas A. Adamts5 deletion blocks murine dermal repair through CD44-mediated aggrecan accumulation and modulation of transforming growth factor beta1 (TGFbeta1) signaling. *J Biol Chem* 2011;286:26016–27.
- [30] Malfait AM, Ritchie J, Gil AS, Austin JS, Hartke J, Qin W, et al. ADAMTS-5 deficient mice do not develop mechanical allodynia associated with osteoarthritis following medial meniscal destabilization. *Osteoarthr Cartil* 2010;18:572–80.
- [31] McCulloch DR, Le Goff C, Bhatt S, Dixon LJ, Sandy JD, Apte SS. Adamts5, the gene encoding a proteoglycan-degrading metalloprotease, is expressed by specific cell lineages during mouse embryonic development and in adult tissues. *Gene Expr Patterns* 2009;9:314–23.
- [32] Gendron C, Kashiwagi M, Lim NH, Enghild JJ, Thogersen IB, Hughes C, et al. Proteolytic activities of human ADAMTS-5: comparative studies with ADAMTS-4. *J Biol Chem* 2007;282:18294–306.
- [33] Bogdanova A, Berzins U, Nikulshin S, Skrastina D, Ezerta A, Legzdina D, et al. Characterization of human adipose-derived stem cells cultured in autologous serum after subsequent passaging and long term cryopreservation. *J Stem Cells* 2014;9:135–48.
- [34] Kuwahara G, Nishinakamura H, Kojima D, Tashiro T, Kodama S. GM-CSF treated F4/80+ BMCs improve murine hind limb ischemia similar to M-CSF differentiated macrophages. *PLoS ONE* 2014;9 [Epub 2014 Sep 9].

- [35] Somanath PR, Kandel ES, Hay N, Byzova TV. Akt1 signaling regulates integrin activation, matrix recognition, and fibronectin assembly. *J Biol Chem* 2007;282:22964–76.
- [36] Monaghan E, Gueorguiev V, Wilkins-Port C, McKeown-Longo PJ. The receptor for urokinase-type plasminogen activator regulates fibronectin matrix assembly in human skin fibroblasts. *J Biol Chem* 2004;279:1400–7.
- [37] Foulcer SJ, Nelson CM, Quintero MV, Kuberan B, Larkin J, Dours-Zimmermann MT, et al. Determinants of versican-V1 proteoglycan processing by the metalloproteinase ADAMTS5. *J Biol Chem* 2014;289:27859–73.
- [38] Glasson SS, Askew R, Sheppard B, Carito B, Blanchet T, Ma HL, et al. Deletion of active ADAMTS5 prevents cartilage degradation in a murine model of osteoarthritis. *Nature* 2005;434:644–8.
- [39] Stanton H, Rogerson FM, East CJ, Golub SB, Lawlor KE, Meeker CT, et al. ADAMTS5 is the major aggrecanase in mouse cartilage in vivo and in vitro. *Nature* 2005;434:648–52.
- [40] Frank JE, Thompson VP, Brown MP, Sandy JD. Removal of O-linked and N-linked oligosaccharides is required for optimum detection of NITEGE neopeptide on ADAMTS4-digested fetal aggrecans: implications for specific N-linked glycan-dependent aggrecanolytic at Glu373–Ala374. *Osteoarthr Cartil* 2009;17:777–81.
- [41] Yasumoto T, B, M, Bird J, Mason R. Species and age-related differences in the turnover of aggrecan and link protein (Abstract). February 1–4, 1999, 45th annual meeting, Orthopaedic Research Society, Anaheim, California; 1999 [24, 82].
- [42] Li J, Anemaet W, Diaz MA, Buchanan S, Tortorella M, Malfait AM, et al. Knockout of ADAMTS5 does not eliminate cartilage aggrecanase activity but abrogates joint fibrosis and promotes cartilage aggrecan deposition in murine osteoarthritis models. *J Orthop Res* 2011;29:516–22.
- [43] Bell R, Li J, Gorski DJ, Bartels AK, Shewman EF, Wysocki RW, et al. Controlled treadmill exercise eliminates chondroid deposits and restores tensile properties in a new murine tendinopathy model. *J Biomech* 2013;46:498–505.
- [44] Gao D, Gu C, Wu Y, Xie J, Yao B, Li J, et al. Mesenchymal stromal cells enhance wound healing by ameliorating impaired metabolism in diabetic mice. *Cytherapy* 2014;16:1467–75.
- [45] Farrell MJ, Shin JI, Smith LJ, Mauck RL. Functional consequences of glucose and oxygen deprivation on engineered mesenchymal stem cell-based cartilage constructs. *Osteoarthr Cartil* 2015;23:134–42.
- [46] Cigan AD, Nims RJ, Albro MB, Esau JD, Dreyer MP, Vunjak-Novakovic G, et al. Insulin, ascorbate, and glucose have a much greater influence than transferrin and selenous acid on the in vitro growth of engineered cartilage in chondrogenic media. *Tissue Eng A* 2013;19:1941–8.
- [47] Tsai WC, Liang FC, Cheng JW, Lin LP, Chang SC, Chen HH, et al. High glucose concentration up-regulates the expression of matrix metalloproteinase-9 and -13 in tendon cells. *BMC Musculoskelet Disord* 2013;14:255.
- [48] Yamamoto K, Troeberg L, Scilabra SD, Pelosi M, Murphy CL, Strickland DK, et al. LRP-1-mediated endocytosis regulates extracellular activity of ADAMTS-5 in articular cartilage. *FASEB J* 2013;27:511–21.
- [49] Brewer PD, Habtemichael EN, Romenskaia I, Mastick CC, Coster AC. Insulin-regulated Glut4 translocation: membrane protein trafficking with six distinctive steps. *J Biol Chem* 2014;289:17280–98.
- [50] Rozanov DV, Hahn-Dantona E, Strickland DK, Strongin AY. The low density lipoprotein receptor-related protein LRP is regulated by membrane type-1 matrix metalloproteinase (MT1-MMP) proteolysis in malignant cells. *J Biol Chem* 2004;279:4260–8.
- [51] Roebroek AJ, Reekmans S, Lauwers A, Feyaerts N, Smeijers L, Hartmann D. Mutant Lrp1 knock-in mice generated by recombinase-mediated cassette exchange reveal differential importance of the NPXY motifs in the intracellular domain of LRP1 for normal fetal development. *Mol Cell Biol* 2006;26:605–16.
- [52] Didangelos A, Mayr U, Monaco C, Mayr M. Novel role of ADAMTS-5 protein in proteoglycan turnover and lipoprotein retention in atherosclerosis. *J Biol Chem* 2012;287:19341–5.
- [53] Dupuis LE, Osinska H, Weinstein MB, Hinton RB, Kern CB. Insufficient versican cleavage and Smad2 phosphorylation results in bicuspid aortic and pulmonary valves. *J Mol Cell Cardiol* 2013;60:50–9.
- [54] McCulloch DR, Nelson CM, Dixon LJ, Silver DL, Wylie JD, Lindner V, et al. ADAMTS metalloproteinases generate active versican fragments that regulate interdigital web regression. *Dev Cell* 2009;17:687–98.
- [55] Ariyoshi W, Knudson CB, Luo N, Fosang AJ, Knudson W. Internalization of aggrecan G1 domain neopeptide ITEGE in chondrocytes requires CD44. *J Biol Chem* 2010;285:36216–24.
- [56] Bell R, Li J, Shewman EF, Galante JO, Cole BJ, Bach Jr BR, et al. ADAMTS5 is required for biomechanically-stimulated healing of murine tendinopathy. *J Orthop Res* 2013;31:1540–8.
- [57] East CJ, Stanton H, Golub SB, Rogerson FM, Fosang AJ. ADAMTS-5 deficiency does not block aggrecanolytic at preferred cleavage sites in the chondroitin sulfate-rich region of aggrecan. *J Biol Chem* 2007;282:8632–40.
- [58] Rogerson FM, Stanton H, East CJ, Golub SB, Tutolo L, Farmer PJ, et al. Evidence of a novel aggrecan-degrading activity in cartilage: Studies of mice deficient in both ADAMTS-4 and ADAMTS-5. *Arthritis Rheum* 2008;58:1664–73.
- [59] Demircan K, Topcu V, Takigawa T, Akyol S, Yonezawa T, Ozturk G, et al. ADAMTS4 and ADAMTS5 knockout mice are protected from versican but not aggrecan or brevican proteolysis during spinal cord injury. *Biomed Res Int*; 2014[Epub 2014 Jul 3].
- [60] Filou S, Stylianou M, Triantaphyllidou IE, Papadas T, Mastronikolis NS, Goumas PD, et al. Expression and distribution of aggrecanases in human larynx: ADAMTS-5/aggrecanase-2 is the main aggrecanase in laryngeal carcinoma. *Biochimie* 2013;95:725–34.
- [61] Plaas A, Osborn B, Yoshihara Y, Bai Y, Bloom T, Nelson F, et al. Aggrecanolytic in human osteoarthritis: confocal localization and biochemical characterization of ADAMTS5-hyaluronan complexes in articular cartilages. *Osteoarthr Cartil* 2007;15:719–34.
- [62] Plaas A, Sandy JD, Liu H, Diaz MA, Schenkman D, Magnus RP, et al. Biochemical identification and immunolocalization of aggrecan, ADAMTS5 and inter-alpha-trypsin-inhibitor in equine degenerative suspensory ligament desmitis. *J Orthop Res* 2011;29:900–6.
- [63] Zhang E, Yan X, Zhang M, Chang X, Bai Z, He Y, et al. Aggrecanases in the human synovial fluid at different stages of osteoarthritis. *Clin Rheumatol* 2013;32:797–803.
- [64] Zeng W, Corcoran C, Collins-Racie LA, Lavallie ER, Morris EA, Flannery CR. Glycosaminoglycan-binding properties and

- aggrecanase activities of truncated ADAMTSs: comparative analyses with ADAMTS-5, -9, -16 and -18. *Biochim Biophys Acta* 2006;1760:517–24.
- [65] Vertel BM, Velasco A, LaFrance S, Walters L, Kaczman-Daniel K. Precursors of chondroitin sulfate proteoglycan are segregated within a subcompartment of the chondrocyte endoplasmic reticulum. *J Cell Biol* 1989;109:1827–36.
- [66] Cross NA, Chandrasekharan S, Jokonya N, Fowles A, Hamdy FC, Buttle DJ, et al. The expression and regulation of ADAMTS-1, -4, -5, -9, and -15, and TIMP-3 by TGFbeta1 in prostate cells: relevance to the accumulation of versican. *Prostate* 2005;63:269–75.
- [67] Lemons ML, Sandy JD, Anderson DK, Howland DR. Intact aggrecan and fragments generated by both aggrecanase and metalloproteinase-like activities are present in the developing and adult rat spinal cord and their relative abundance is altered by injury. *J Neurosci* 2001;21:4772–81.
- [68] Demircan K, Yonezawa T, Takigawa T, Topcu V, Erdogan S, Ucar F, et al. ADAMTS1, ADAMTS5, ADAMTS9 and aggrecanase-generated proteoglycan fragments are induced following spinal cord injury in mouse. *Neurosci Lett* 2013;544:25–30.
- [69] Ilic MZ, Vankemmelbeke MN, Hohen I, Buttle DJ, Clem Robinson H, Handley CJ. Bovine joint capsule and fibroblasts derived from joint capsule express aggrecanase activity. *Matrix Biol* 2000;19:257–65.
- [70] Boeuf S, Graf F, Fischer J, Moradi B, Little CB, Richter W. Regulation of aggrecanases from the ADAMTS family and aggrecan neopeptide formation during in vitro chondrogenesis of human mesenchymal stem cells. *Eur Cell Mater* 2012;23:320–32.
- [71] Viapiano MS, Hockfield S, Matthews RT. BEHAB/brevican requires ADAMTS-mediated proteolytic cleavage to promote glioma invasion. *J Neurooncol* 2008;88:261–72.
- [72] Malfait AM, Amer EC, Song RH, Alston JT, Markosyan S, Staten N, et al. Proprotein convertase activation of aggrecanases in cartilage in situ. *Arch Biochem Biophys* 2008;478:43–51.
- [73] Dancevic CM, Fraser FW, Smith AD, Stupka N, Ward AC, McCulloch DR. Biosynthesis and expression of a disintegrin-like and metalloproteinase domain with thrombospondin-1 repeats-15: a novel versican-cleaving proteoglycanase. *J Biol Chem* 2013;288:37267–76.
- [74] Little CB, Mittaz L, Belluocci D, Rogerson FM, Campbell IK, Meeker CT, et al. ADAMTS-1-knockout mice do not exhibit abnormalities in aggrecan turnover in vitro or in vivo. *Arthritis Rheum* 2005;52:1461–72.
- [75] Collins-Racie LA, Flannery CR, Zeng W, Corcoran C, Annis-Freeman B, Agostino MJ, et al. ADAMTS-8 exhibits aggrecanase activity and is expressed in human articular cartilage. *Matrix Biol* 2004;23:219–30.
- [76] Choi GC, Li J, Wang Y, Li L, Zhong L, Ma B, et al. The metalloprotease ADAMTS8 displays antitumor properties through antagonizing EGFR-MEK-ERK signaling and is silenced in carcinomas by CpG methylation. *Mol Cancer Res* 2014;12:228–38.
- [77] Dubail J, Aramaki-Hattori N, Bader HL, Nelson CM, Katebi N, Matuska B, et al. A new Adamts9 conditional mouse allele identifies its non-redundant role in interdigital web regression. *Genesis* 2014;52:702–12.
- [78] Shibata S, Fukada K, Imai H, Abe T, Yamashita Y. In situ hybridization and immunohistochemistry of versican, aggrecan and link protein, and histochemistry of hyaluronan in the developing mouse limb bud cartilage. *J Anat* 2003;203:425–32.
- [79] Koo BH, Apte SS. Cell-surface processing of the metalloprotease pro-ADAMTS9 is influenced by the chaperone GRP94/gp96. *J Biol Chem* 2010;285:197–205.
- [80] Koo BH, Longpre JM, Somerville RP, Alexander JP, Leduc R, Apte SS. Regulation of ADAMTS9 secretion and enzymatic activity by its propeptide. *J Biol Chem* 2007;282:16146–54.
- [81] Coughlan TC, Crawford A, Goldring MB, Hatton PV, Barker MD. Lentiviral shRNA knock-down of ADAMTS-5 and -9 restores matrix deposition in 3D chondrocyte culture. *J Tissue Eng Regen Med* 2010;4:611–8.
- [82] Nicholson AC, Malik SB, Logsdon Jr JM, Van Meir EG. Functional evolution of ADAMTS genes: evidence from analyses of phylogeny and gene organization. *BMC Evol Biol* 2005;5:11.
- [83] Jedrychowski MP, Gartner CA, Gygi SP, Zhou L, Herz J, Kandror KV, et al. Proteomic analysis of GLUT4 storage vesicles reveals LRP1 to be an important vesicle component and target of insulin signaling. *J Biol Chem* 2010;285:104–14.
- [84] Chen TL, Wang PY, Luo W, Gwon SS, Flay NW, Zheng J, et al. Aggrecan domains expected to traffic through the exocytic pathway are misdirected to the nucleus. *Exp Cell Res* 2001;263:224–35.
- [85] Zheng J, Luo W, Tanzer ML. Aggrecan synthesis and secretion. A paradigm for molecular and cellular coordination of multiglobular protein folding and intracellular trafficking. *J Biol Chem* 1998;273:12999–3006.
- [86] Kossi J, Laato M. Different metabolism of hexose sugars and sucrose in wound fluid and in fibroblast cultures derived from granulation tissue, hypertrophic scar and keloid. *Pathobiology* 2000;68:29–35.
- [87] Wang A, Hascall VC. Hyaluronan structures synthesized by rat mesangial cells in response to hyperglycemia induce monocyte adhesion. *J Biol Chem* 2004;279:10279–85.
- [88] Jokela TA, Jauhiainen M, Auriola S, Kauhanen M, Tiihonen R, Tammi M, et al. Mannose inhibits hyaluronan synthesis by down-regulation of the cellular pool of UDP-N-acetylhexosamines. *J Biol Chem* 2008;283:7666–73.
- [89] Wang A, Midura RJ, Vasanji A, Wang AJ, Hascall VC. Hyperglycemia diverts dividing osteoblastic precursor cells to an adipogenic pathway and induces synthesis of a hyaluronan matrix that is adhesive for monocytes. *J Biol Chem* 2014;289:11410–20.
- [90] Wang A, de la Motte C, Lauer M, Hascall V. Hyaluronan matrices in pathological processes. *FEBS J* 2011;278:1412–8.
- [91] Kopesky PW, Lee HY, Vanderploeg EJ, Kisiday JD, Frisbie DD, Plaas AH, et al. Adult equine bone marrow stromal cells produce a cartilage-like ECM mechanically superior to animal-matched adult chondrocytes. *Matrix Biol* 2010;29:427–38.
- [92] Pazdro R, Harrison DE. Murine adipose tissue-derived stromal cell apoptosis and susceptibility to oxidative stress in vitro are regulated by genetic background. *PLoS ONE* 2013;8:e61235.
- [93] Gosset M, Berenbaum F, Thirion S, Jacques C. Primary culture and phenotyping of murine chondrocytes. *Nat Protoc* 2008;3:1253–60.
- [94] Oshita H, Sandy JD, Suzuki K, Akaike A, Bai Y, Sasaki T, et al. Mature bovine articular cartilage contains abundant aggrecan that is C-terminally truncated at Ala719–Ala720, a site which is readily cleaved by m-calpain. *Biochem J* 2004;382:253–9.
- [95] Sandy JD, Westling J, Kenagy RD, Iruela-Arispe ML, Verscharen C, Rodriguez-Mazaneque JC, et al. Versican V1 proteolysis in human aorta in vivo occurs at the Glu441–

- Ala442 bond, a site that is cleaved by recombinant ADAMTS-1 and ADAMTS-4. *J Biol Chem* 2001;276:13372–8.
- [96] Calabro A, Midura R, Wang A, West L, Plaas A, Hascall VC. Fluorophore-assisted carbohydrate electrophoresis (FACE) of glycosaminoglycans. *Osteoarthr Cartil* 2001;9:S16–22 Suppl. A.
- [97] Kim YJ, Sah RL, Doong JY, Grodzinsky AJ. Fluorometric assay of DNA in cartilage explants using Hoechst 33258. *Anal Biochem* 1988;174:168–76.
- [98] Stewart MC, Fosang AJ, Bai Y, Osborn B, Plaas A, Sandy JD. ADAMTS5-mediated aggrecanolytic activity in murine epiphyseal chondrocyte cultures. *Osteoarthr Cartil* 2006;14:392–402.
- [99] Ripellino JA, Klinger MM, Margolis RU, Margolis RK. The hyaluronic acid binding region as a specific probe for the localization of hyaluronic acid in tissue sections. Application to chick embryo and rat brain. *J Histochem Cytochem* 1985;33:1060–6.